의학박사 학위논문

Identification and exploration of novel biomarkers for CYP3A activity using global metabolomics

비표적 대사체학을 이용한 새로운 CYP3A 활성능 예측 바이오마커 동정 및 탐색

2018 년 1 월

서울대학교 대학원
의과학과 의과학전공
김 보 라

A thesis of the Degree of Doctor of Philosophy

비표적 대사체학을 이용한 새로운 CYP3A 활성능 예측 바이오마커 동정 및 탐색

Identification and exploration of novel biomarkers for CYP3A activity using global metabolomics

January 2018

The Department of Biomedical Sciences,
Seoul National University
College of Medicine
Bora Kim

비표적 대사체학을 이용한 새로운 CYP3A 활성능 예측 바이오마커 동정 및 탐색

지도 교수 유 경 상

이 논문을 의학박사 학위논문으로 제출함
2018년 1월

서울대학교 대학원
의과학과 의과학전공
김 보 라

김보라의 의학박사 학위논문을 인준함
2018년 1월

위 원 장 _____ (인)
부위원장 _____ (인)
위 원 _____ (인)
위 원 _____ (인)
위 원 _____ (인)

Identification and exploration of novel biomarkers for CYP3A activity using global metabolomics

by
Bora Kim

A thesis submitted to the Department of Biomedical Sciences in partial fulfillment of the requirements for the Degree of Doctor of Philosophy in Medicine at Seoul National University College of Medicine

January 2018

Approved by Thesis Committee:

Professor _____ **Chairman**

Professor _____ **Vice chairman**

Professor _____

Professor _____

Professor _____

ABSTRACT

Introduction: The measurement of cytochrome P450 (CYP)3A activity has been quantitatively assessed using midazolam, which is a specific exogenous probe drug. To avoid unnecessary drug exposure and invasive sampling, evaluating an individual's CYP3A phenotype through measurement of sensitive endogenous biomarkers, especially urinary compounds, would be ideal. Quantitative models of endogenous metabolites are useful in predicting CYP3A-mediated drug–drug interactions. This study aimed to identify novel predictive markers for the magnitude of CYP3A induction and inhibition in male and female subjects.

Methods: Twenty-four Korean male and 12 female volunteers aged 20–50 years were received intravenous midazolam during 3 study phases: phase 1, the control phase, in which we evaluated midazolam Pharmacokinetics (PK); phase 2, the CYP3A-inhibition phase, in which we explored the changes in midazolam PK caused by pretreatment with ketoconazole; and phase 3, the CYP3A-induction phase, in which we assessed the effects of pretreatment with rifampicin on midazolam PK. Their 12-h interval urine samples in each phase were analyzed for global metabolomics using ultra-performance liquid chromatography time-of-flight mass spectrometry. To identify endogenous metabolic markers associated with CYP3A inhibition and induction, we selected metabolic features that satisfied the following conditions in male or female subjects: (1) fold-change of mean relative intensity in inhibition versus control phase < 0.5, (2) fold-change of mean relative intensity in induction

versus control phase > 2.0, and (3) correlation between relative intensity of the compound and midazolam clearance (Pearson's r > 0.7). To assess the enzyme kinetics, recombinant enzymes of CYP3A4, CYP4A11, and CYP4F2 were used, and Km, Vmax, and Vmax/Km values were compared.

Results: We report five ω- or (ω-1)-hydroxylated medium-chain acylcarnitines as novel CYP3A4 markers. Recombinant enzyme assays were used to determine the ω- and (ω-1)-hydroxylation activities of CYP3A4, CYP4A11, and CYP4F2. CYP3A4 catalyzed ω- and (ω-1)-hydroxylated MCFAs with the lowest Km and highest Vmax/Km values. Finally, we derived a model to predict midazolam clearance using these markers and demonstrated that the predictive model including three ω- or (ω-1)-hydroxylated medium-chain acylcarnitines, 6β-OH cortisol, and gender as covariates shows reliable predictability ($r^2 = 0.911$).

$$\begin{aligned}\text{Ln(clearance)} = {} & 1.4443 - 0.5559 \cdot \text{gender}^{\dagger} + 0.1637 \cdot \ln(\text{Car C8:1-OH II/Cr} + 1) \\ & + 0.09661 \cdot \ln(\text{Car C10:2-OH/Cr}+1) + 0.1261 \cdot \ln(\text{Car C11:2-OH/Cr} + 1) \\ & + 0.1191 \cdot \ln(6\beta\text{-OH cortisol/Cr} + 1)\end{aligned}$$

†male = 0, female = 1

Conclusions: Using a global metabolomics approach, we identified urinary hydroxy acylcarnitines as novel CYP3A biomarkers and found that CYP3A4 efficiently catalyzes the ω- and (ω-1)-hydroxylation of MCFAs. The selected markers of hepatic CYP3A activity and the proposed model can be applied to predict DDI mediated by CYP3A.

* Part of this work has been published in Clinical Pharmacology and Therapeutics (Bora Kim, et al. *CPT* In press. doi: 10.1002/cpt.856).

Keywords: CYP3A, drug-drug interaction, quantitative model,

global metabolomics, acylcarnitine, MCFA, ω- and (ω-1)-hydroxylation

Student number: 2013-30608

CONTENTS

LIST OF TABLES

LIST OF FIGURES

LIST OF ABBREVIATION

MCFAs	medium chain fatty acids
CYP	cytochrome P450
DDI	drug-drug interaction
PK	pharmacokinetics
PCA	principal component analysis
QC	quality control
Car C8:1-OH	hydroxy octenoylcarnitine
Car C10:2-OH	hydroxy decadienoylcarnitine
Car C11:2-OH	hydroxy undecadienoylcarnitine
Car C11:1-OH	hydroxy undecenoylcarnitine
16α-OH TS	16α-hydroxy testosterone sulfate
16α-OH AS	16α-hydroxy androsterone sulfate
IC_{50}	half-maximal inhibitory concentration
Cr	creatinine
MCT	medium-chain triacylglycerols
SULT	sulfotransferase
UPLC	ultra-performance liquid chromatography
TOF-MS	time-of-flight mass spectrometry

INTRODUCTION

Human cytochrome P450 (CYP)3A, the most important drug-metabolizing enzyme, accounts for ~40% of total CYP proteins in human liver microsomes and metabolizes more than 50% of the clinically used drugs [1, 2]. The expression of CYP3A4 exhibits a high level of interindividual variation. The major CYP3A isoform, CYP3A4, which is highly expressed in the liver and intestine, has several genotypes, including CYP3A4*18 and CYP3A4*22, that can alter the protein levels or enzyme activity of CYP3A [3, 4]. CYP3A5 is expressed in most Africans but in few Caucasians and Asians. The frequency of the functional CYP3A5*1 allele is present in 14% of Swedes, 33% of Koreans, and 74% of Tanzaniams [5]. The expression of CYP3A enzymes is controlled by nuclear receptors, including the pregnane X receptor, the vitamin D receptor, and retinoid X receptor α [6-8]. Furthermore, different levels of regulation including environmental, hormonal, or nutritional influences cause high interindividual variation in CYP3A activity. Despite of its clinical importance, genetic variants of CYP3A can explain only a small part of interindividual variability of CYP3A activity.

Pharmacokinetic drug–drug interaction (DDI) can lead to serious adverse events; therefore, the evaluation of DDI such as CYP3A-mediated induction or inhibition is important for drug development and in clinical practice because of the growing use of polypharmacy. CYP3A has become one of the recommended enzymes for routine assessment of potential drug interactions using *in vitro* and *in vivo* methodologies [9].

The measurement of CYP3A activity, including inhibition and induction, has been quantitatively assessed using midazolam, which is a specific exogenous probe drug. To avoid unnecessary drug exposure and invasive sampling, evaluating an individual's CYP3A phenotype through measurement of sensitive endogenous biomarkers, especially urinary compounds, would be ideal. Urinary 6β-hydroxycortisol-to-cortisol and 6β-hydroxycortisone-to-cortisone ratios have been suggested as endogenous CYP3A markers and reportedly highly correlate with midazolam clearance *in vivo* [10, 11]. Plasma 4β-hydroxycholesterol has been also evaluated as a surrogate for midazolam pharmacokinetics (PK) [12]. However, intra- and inter-individual variations in 6β-hydroxycortisol are large because of several factors, such as stress, infections, and circadian rhythm [13, 14]. Additionally, studies have demonstrated that plasma free cortisol and 6β-hydroxycortisol are filtered through the renal glomeruli and partially reabsorbed via the tubules; thus, urinary 6β-hydroxycortisol and its ratio to cortisol are affected by the renal function of individuals [15, 16]. The elimination half-life of 4β-hydroxycholesterol reportedly ranges from 60 h to 17 days [17, 18], resulting in a limited dynamic range for assessment of CYP3A inhibition status. Recent CYP3A biomarkers are serum 4β,25-dihydroxyvitamin D3 [19] and urinary 1β-hydroxy-deoxycholic acid [20], which are still to be validated *in vivo*. Therefore, a new sensitive endogenous biomarker, which is preferably measureable in urine samples but does not depend on renal clearance, is needed for the assessment of DDI and for phenotyping CYP3A activity.

Metabolomics analyses can be broadly classified into targeted and global

approaches. In targeted approaches, a preselected subset of metabolites belonging to defined chemical classes or typical metabolic pathways are quantified. In the global profiling approach, a multitude of metabolites are quantified without any preselection. This approach is advantageous to identify novel biomarkers or to generate hypotheses in exploratory studies. To date, CYP3A biomarkers have been evaluated only by targeted metabolomics. Using targeted steroid profiling, we previously reported models for predicting midazolam clearance based on 7β-OH DHEA/DHEA, 6β-OH cortisol/cortisol, and 6β-OH cortisone/cortisone in male [10] and female [11] subjects. Furthermore, we validated major steroid markers and developed the model in various sex- and age-stratified groups at the basal state [21].

Here, we aimed to evaluate new metabolic markers associated with the inhibition and induction of CYP3A activity in human urine using global metabolomics for the first time. Furthermore, we generated a predictive model for predicting midazolam clearance based on the newly identified metabolite markers for CYP3A-mediated DDIs in both male and female subjects.

METHODS

Study design

The open-label, fixed-sequence, three-treatment, three-period clinical studies conducted in the Clinical Trials Center of Seoul National University Hospital (SNUH), Seoul, Republic of Korea on male (4) and female (5) subjects have been reported. The protocol was approved by the Institutional Review Board at SNUH. All procedures were conducted in accordance with the principles of the Declaration of Helsinki (59th World Medical Association General Assembly, Seoul, October 2008) and Good Clinical Practice (GCP) guidelines, Before starting subject enrollment, this trial was registered in a public trial registry, ClinicalTrials.gov (http://www.clinicaltrials.gov; identifier no. NCT01760642, NCT01215214).

Each subject received intravenous midazolam during 3 study phases: phase 1, the control phase, in which we evaluated midazolam PK (i.v., 1 mg); phase 2, the CYP3A-inhibition phase, in which we explored the changes in midazolam (i.v., 1 mg) PK caused by pretreatment with a 400-mg oral dose of ketoconazole once daily for 4 days; and phase 3, the CYP3A-induction phase, in which we assessed the effects of pretreatment with 600 mg oral rifampicin once daily for 10 days on midazolam (i.v., 2.5 mg) PK. To minimize the effect of menstrual cycle on steroid levels, the 3 phases in women volunteers were separated by individual menstruation cycles; midazolam was administered at the same phase of the cycle for each subject. Details on enrollment of female subjects have been reported (34). For metabolomics

analyses, urine samples were collected at 12-h intervals during each study period, 24 h before midazolam administration.

Subjects

Healthy Korean male and female volunteers aged 20–50 years were eligible for participation in this trial if they had body mass indexes of 17.0–28.0 kg/m2, and weighed over 50 kg for males and 45–85 kg for females. All subjects agreed to use contraception during the study and provided written informed consent before being screened. Subjects were judged healthy based on medical history, physical examination, vital signs, 12-lead electrocardiography, serology (hepatitis B surface antigen, anti-hepatitis C virus, and anti-HIV), and routine clinical laboratory tests (clinical chemistry, hematology, and urinalysis). Any subjects who had ingested any drugs within 2 weeks of the first drug intake were excluded. Consumption of grapefruit and grapefruit products was not permitted from 7 days before the first drug administration until the final day of the study.

Chemicals and reagents

Formic acid and sulfatase (type H-1 from Helix pomatia) were purchased from Sigma-Aldrich (St. Louis, MO). HPLC-grade solvents (methanol, acetonitrile and water) were purchased from J.T. Baker (Center Valley, PA). Semi-quantified acylcarnitines (octanoyl and decanoyl carnitine) and fatty acids (octanoic, 2-octenoic, 3-octenoic, 7-octenoic, and 8-hydroxyoctanoic

acid) for in vitro microsome studies were obtained from Sigma-Aldrich. Internal standards, octanoic-2,2-d2 acid, octanoyl-L-carnitine-d3, decanoyl-L-carnitine-d3, cortisol-d4, testosterone sulfate-d3, and Cr-d4 were purchased from CDN isotopes (Pointe-Claire, Quebec, Canada). Supersomes containing CYP enzymes coexpressed with CYP reductase and cytochrome b5 (except CYP 4A11) were purchased from Corning (Woburn, MO). The activity of supersomes is catalyzed by each CYP enzymes which is expressed from human CYP3A4 cDNA using a baculovirus expression system. For solid-phase extraction, an Oasis HLB cartridge (3 mL, 60 mg; Waters, Milford, MA) was used.

Pharmacogenetic assessments

TaqMan SNP genotyping assays (CYP3A5*3 A6956G and NR1I2 C-25385T) were carried out using TaqMan Genotyping Assays (Applied Biosystems, Foster City, CA) and a 7500 Real-Time PCR system (Applied Biosystems) as previously described (5).

Global metabolomics

Urine samples were thawed on ice and centrifuged at 15,000 ×g for 20 min at 4 °C to remove particles. The supernatant was diluted with 2 volumes of water. A 3-µL aliquot of the sample was injected onto a reverse-phase 2.1 × 100 mm ACQUITY 1.8-µm HSS T3 column using a Waters ultra-performance liquid chromatography (UPLC) system. The gradient mobile

phase comprised 0.1% formic acid (A) and methanol containing 0.1 formic acid (B). Each sample was resolved for 20 min at a flow rate of 0.4 mL/min. The gradient consisted of 5% B for 1 min, 5–30% B over 1–8 min, 30–70% B over 8–13 min, and 95% B for 14 min maintaining for 2 min. The samples were equilibrated at 95% A for 3.5 min before the next injection. A Waters Xevo G2 time-of-flight mass spectrometry (QTOF-MS) was operated in positive and negative ionization modes. The QTOF (Waters Corp) was operated in both the positive ion and negative ion electrospray ionization mode. The capillary and cone voltages were maintained at 3 kV and 40 V, respectively. Nitrogen was used as both a desolvation gas (900 L/h) and a cone gas (30 L/h). The source and desolvation temperatures were set at 120 and 450 °C, respectively. The QTOF was calibrated with sodium formate solution (range, m/z 50–1200) to ensure mass accuracy and was monitored using a lock mass, leucine enkephaline, in real time. To obtain consistent differential variables, a pooled urine sample (QC) was prepared by mixing aliquots of individual samples. Replicates of the QC sample were acquired in a series of injections, and data were obtained by random injection. Chromatographic mass data were aligned, and the ketoconazole and rifampicin metaboliteswere removed using MarkerLynx (Waters Corp.). The parameters of the MarkerLynx method were set as follows: mass tolerance, 0.05 Da; noise elimination level, 6; employment of the full-scan mode in the mass range of 100–900 amu; and initial and final retention times of 0.5 and 16 min, respectively, for data collection. All data were normalized to the sum of the total ion intensity per chromatogram, and the resultant data were imported

into EZinfo 2.0 software (Umetrics, Umea, Sweden) for multivariate analysis (pareto-scaled). PCA was used to examine the intrinsic variation within a group and to assess the clustering behavior between groups.

Identification of CYP3A biomarkers

The elemental composition of ions was investigated further by MS fragmentation, database searching, deconjugation of urinary metabolites, and confirmation using authentic standards, with MassLynx software. In addition, the Human Metabolome Database (HMDB, http://www.hmdb.ca/) and Metlin Database (https://metlin.scripps.edu/index.php) were used for mass-based identification searches. Metabolites that had a fragmentation pattern of sulfate conjugation were enzymatically deconjugated, and the free form of each metabolite was identified by MS fragmentation. Sulfated compounds have fragmentation peaks at m/z 96.96 in the negative-ion mode. The deconjugation system for urinary metabolites contained the following: 1 mL of urine, 50 μL of β-glucuronidase/arylsulfatase, and 500 μL of phosphate buffer (pH 7.4). A blank sample containing buffer instead of enzymes was used as a control. The mixtures were incubated for 20 h at 40°C. After centrifuged at 14,000 rpm for 5 min, the supernatant were extracted with Oasis HLB solid-phase extraction cartridges coupled to a peristaltic pump. After loading a sample onto a cartridge, the cartridge was washed with 3 mL of water and eluted twice with 2 mL of methanol. The combined methanol eluates were evaporated under nitrogen at room temperature and the dried

residue was reconstituted with 100 μL of methanol. Four-microliter aliquots were injected into the UPLC-QTOF system.

Quantification of CYP3A biomarkers

Five endogenous acylcarnitines, C8:1-OH I, C8:1-OH II, C10:2-OH, C11:2-OH, and C11:1-OH, and 6β-OH cortisol, 16α-OH TS, and 16α-OH AS were (semi-)quantified using TargetLynx (Waters Corp.) In the absence of reference standards of unsaturated or hydroxy acylcarnitines, the related saturated acylcarnitines, i.e. carnitine C8:0 for carnitines of C8:1-OH 1 and C8:1-OH 2, and carnitine C10:0 for carnitines C10:2-OH, C11:2-OH, and 11:1-OH, were used for preparing standard curves. Cr was quantified for normalization to determine actual biomarker concentrations. Fifty microliters of urine supernatant was diluted in 150 μL of five international standard mixtures: 500 ng/mL of carnitine C8:0-d3, carnitine C10:0-d3, testosterone sulfate-d3, 600 ng/mL of cortisol-d4, and 1 μg/mL of Cr-d3. The concentration of each biomarker in the urine was determined from the calibration curves using linear regression analysis. All determined correlation coefficients were >0.98 for each biomarker, and the resultant concentrations were expressed as ng/mg Cr (normalized).

Microsomal incubations

All samples were processed in duplicate. Octenoic acid dissolved in acetonitrile was added to a reaction mixture (final volume 100 μL) containing 1.4 mM NADPH and 20 pmol CYP3A4, CYP4A11, or CYP4F2 supersomes

in phosphate buffer (pH 7.4). The reactions were initiated by the addition of NADPH (final concentration of 1.5 mmol/L) and quenched after 1-h incubation at 37°C by adding 300 μL of 500 ng/mL octanoic acid-d2 in methanol. Km and Vmax for hydroxy-2-octenoic acid in supersomes were determined using 2-octenoic acid concentrations of 0.1, 0.2, 0.5, 1.0, 2.5, 5.0, and 10.0 mmol/L. The IC50 value for ketoconazole in supersomes was measured using hydroxy-2-octenoic acid formation from 2.5 mm of 2-octenoic acid and ketoconazole at 0 (Acetonitrile vehicle control), 10, 50, 125, 250, 500, 1000, and 2000 μmol/L. For semi-quantitation of ω- and (ω-1)-hydroxy-2-octenoic acid, the calibration curve of 8-hydroxy octanoic acid was constructed between 6 ng/mL and 6,500 ng/mL.

Data and statistical analyses

PK parameters and demographic characteristics were analyzed using descriptive statistics. The effects of two genotypes (CYP3A5 and NR1I2) on PK parameters and demographic characteristics were analyzed using analysis of variance. Gender, genotype, and all metabolites that correlated with midazolam clearance were evaluated as variables in the mixed effects model with random subject effect to account for the repeated measures. We selected the significant predictors in the model using backward elimination based on the lowest Akaike's information criterion value. Statistical analysis of mixed model was performed using the mixed procedure (SAS v. 9.3). The mixed model generalizes the standard linear model as follows:

$$y = X\beta + Z\gamma + \varepsilon.$$

In this expression, y represents a vector of observed data, β is a vector of parameters associated with the fixed factors with known design matrix X, γ is a vector of random effects with known design matrix Z, and ε is an unknown random error vector whose elements are not required to be independent or homogeneous. Endogenous metabolites were analyzed using the mixed-effects model with treatment (inhibition, control, and induction), genotype, gender as the fixed effect and subject as the random effect on log-transformed metabolite concentrations. Considering that some metabolites were below the LLOQ in several subjects, we used the value of ln(Cr-normalized metabolite concentration +1) for variables. Previous steroid markers (6β-OH cortisol/cortisol and 6β-OH cortisone/cortisone) found in healthy male and female integrated model [22] and age (known as a CYP3A-associated factor [23]) were combined with acylcarnitine markers in this study to compare and integrate the results, as described in the "DISCUSSION" section. All statistical analyses were performed using SAS v. 9.3 (SAS Institute, Cary, NC).

Km and Vmax for hydroxylation of 2-octenoic acid in CYP3A4, CYP4A11, and CYP4F2 supersomes were obtained by fitting the Michaelis-Menten equation to the data, using GraphPad Prism (La Jolla, CA). IC50 values were obtained using a sigmoid dose-response (inhibition) model.

RESULTS

Subjects

In this study, 26 male and 16 female healthy subjects were enrolled, but 2 male and 4 female subjects withdrew informed consent, leaving 24 male and 12 female subjects who completed the study (**Table 1** for demographics). The male subjects were 20–38 years of age (mean ± SD, 26.5 ± 4.6 years) and weighed 56.8–87.3 kg (mean ± SD, 69.2 ± 7.7 kg). The female subjects were 20–30 years of age (mean ± SD, 23.9 ± 4.1 years) and weighed 46.0–59.6 kg (mean ± SD, 51.3 ± 4.4 kg). PK and metabolomics were analyzed for subjects who completed the study. No serious or unpredictable adverse events were observed.

Table 1. Demographics of subjects

Item	Male (Mean [range])	Female (Mean [range])
N	24	12
Age (year)	26.5 [20-38]	23.9 [20-30]
Height (m)	1.75 [1.67-1.92]	1.61 [1.52-1.68]
Weight (kg)	69.2 [56.8-87.3]	51.3 [46.0-59.6]

PK of midazolam

PK parameters of midazolam were used as the gold standard for predicting CYP3A activity. Descriptive statistics of the midazolam PK parameters according to treatment are shown in **Table 2**. After ketoconazole treatment (inhibition phase), the mean clearance of midazolam decreased to ~30% and ~20% as compared to the mean clearance after midazolam treatment alone (control phase) in male and female subjects, respectively. Mean midazolam clearance increased more than 2-fold after rifampicin treatment (induction phase) as compared to the control phase in both genders. PK parameters did not differ between the CYP3A5 genotype and NR1I2 genotype during the three phases (analysis of variance, $P > 0.05$).

Table 2. Pharmacokinetic parameters after a single intravenous administration of midazolam alone or concomitant dose with steady-state ketoconazole or rifampicin

Parameter	Midazolam alone		Midazolam + ketoconazole		Midazolam + rifampicin	
	Male	Female	Male	Female	Male	Female
AUC_{inf}/dose (ng·h/mL/mg)	36.21 ± 11.47	43.22 ± 8.29	102.54 ± 22.48	211.58 ± 42.97	16.15 ± 3.08	21.56 ± 3.80
GMR (90s% CI)	-	-	2.89 (2.57-3.25)	4.77 (4.52-5.03)	0.46 (0.41-0.51)	0.49 (0.46-0.53)
Clearance (L/h)	30.08 ± 9.04	23.1 ± 4.26	10.26 ± 2.59	5.01 ± 1.19	64.16 ± 12.44	47.8 ± 9.05
Vd (L)	170.1 ± 18.3	131.0 ± 23.8	142.2 ± 11.1	55.0 ± 6.14	249.1 ± 12.6	196.9 ± 62.2
$t_{1/2}$ (h)	3.92 ± 1.40	3.98 ± 0.72	9.61 ± 2.98	7.88 ± 1.52	2.69 ± 0.70	2.93 ± 1.01

AUC_{inf}, area under the plasma concentration vs. time curve extrapolated to infinity

GMR, geometric mean ratio of AUC_{inf}/dosea

CI, confidence interval

Vd, volume of distribution

$t_{1/2}$, terminal half-life.

Genotype results

CYP3A5*3 (A6956G) and NR1I2 (C-25385T) genotypes of 24 subjects were listed in Table 3. Frequencies for CYP3A5*3 and NR1I2 genotypes were indicated in **Table 3**. Minor allele frequency for CYP3A5*3 and NR1I2 in both male and female were consistent with previously reports.

Table 3. Frequencies of CYP3A5*3 and NR1I2 genotypes in male and female subjects

Item	CYP3A5*3 (**A6956G, rs776746)**				NR1I2 (**C-25385T, rs3814055)**			
	AA	AG	GG	MAF	CC	CT	TT	MAF
Male (**Mean [range])**	-	10	14	0.792	10	14	-	0.292
Female **(Mean [range])**	1	3	8	0.792	5	5	2	0.375

*MAF: minor allele frequency

Global metabolome analysis

Urine samples from the inhibition, control, and induction phases were analyzed by UPLC-QTOF operated in positive and negative ionization modes. **Figure 1** shows the selection procedure of markers reflecting CYP3A activity. In total, 7,535 ions were produced in positive and negative modes using MarkerLynx. To remove metabolites of ketoconazole or rifampicin and select endogenous markers with good intensity, we eliminated ions if >20% of all subjects in all phases had zero intensity, leaving 6,056 ions that were subjected to multivariate analysis. After data normalization, principal component analysis (PCA) was used to classify the metabolic phenotypes. Unsupervised PCA clearly differentiated the three phases in both male and female subjects (**Figure 2**). Clustering of quality control (QC) samples in PCA demonstrated platform stability and reproducibility. To identify endogenous metabolic markers associated with CYP3A inhibition and induction, we selected metabolic features that satisfied the following conditions in male or female subjects (**Figure 1**): (1) fold-change of mean relative intensity in inhibition *versus* control phase < 0.5, (2) fold-change of mean relative intensity in induction *versus* control phase > 2.0, and (3) correlation between relative intensity of the compound and midazolam clearance (Pearson's r > 0.7). Eighteen features were selected as potential CYP3A biomarkers and adducts were organized by retention time and fragmentation pattern (**Table 4**).

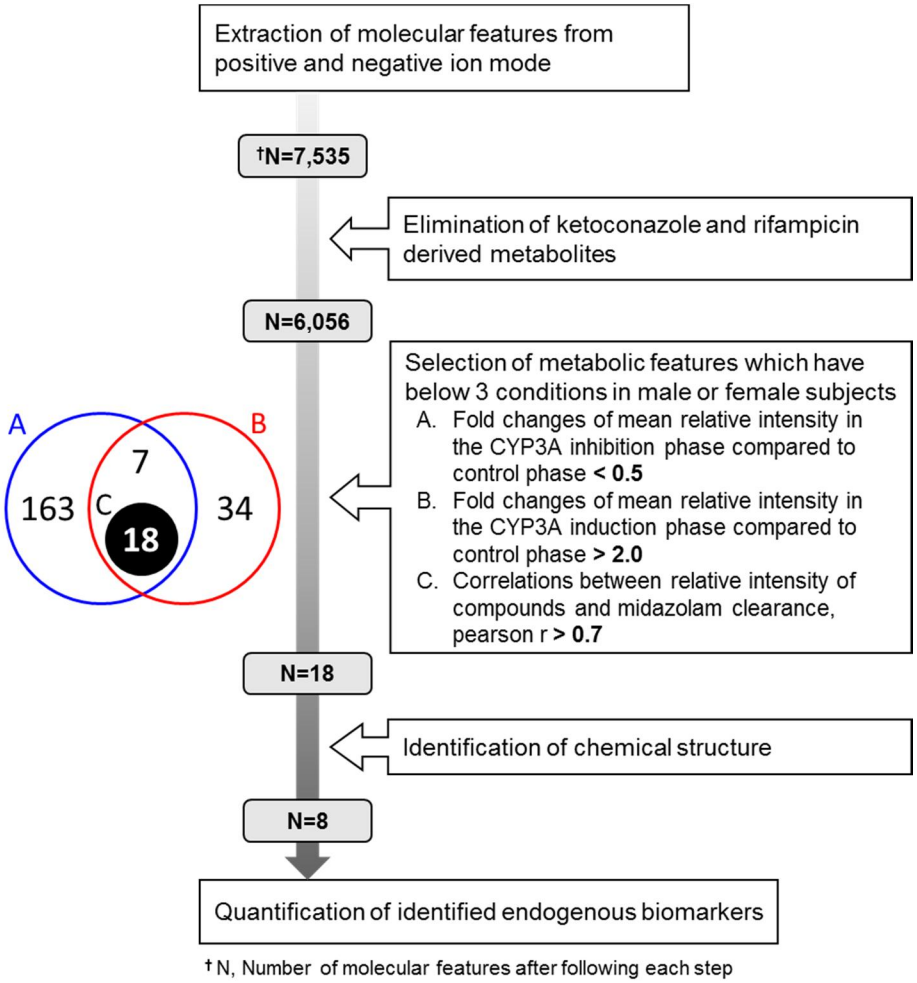

Figure 1. Scheme of the untargeted metabolomics strategy to determine urinary biomarkers reflecting CYP3A activity.

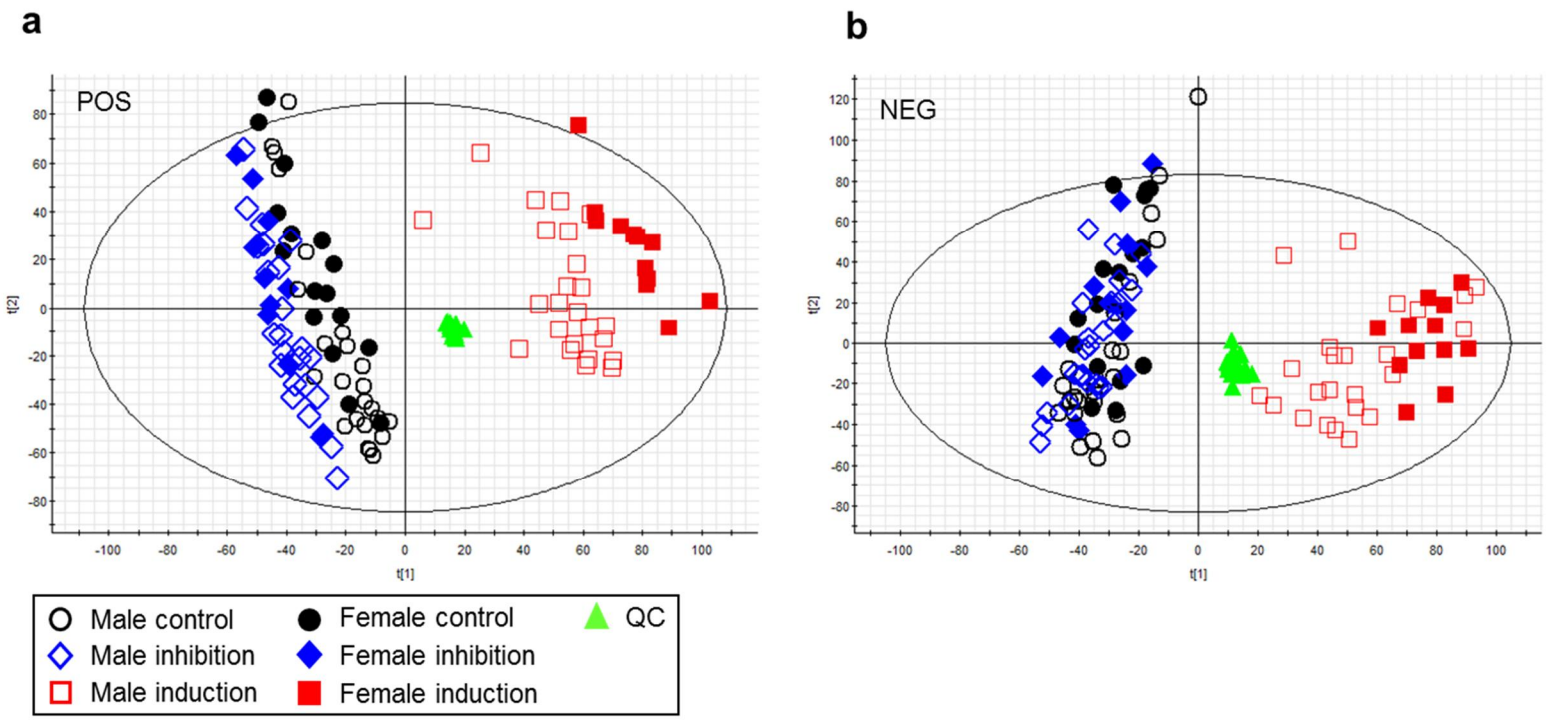

Figure 2. PCA score plots derived from UPLC-TOF MS untargeted analysis of the control, inhibition, and induction groups of male and female subjects in (a) positive- and (b) negative-ion modes.

Table 4. Identified urinary CYP3A biomarkers and their fold-changes of mean relative intensity in the CYP3A inhibition and induction phases *versus* the control phase, and correlation with midazolam clearance

Metabolites	RT (min)	Mass (*m/z*)	Fold-change in males		Fold-change in females		Correlation with midazolam clearance	
			Inhibition phase	Induction phase	Inhibition phase	Induction phase	r	*P*
Car C8:1-OH I	4.93	302.1962†	▼ 0.54	▲ 3.67	▼ 0.30	▲ 2.99	0.82	< 0.001
Car C8:1-OH II	5.14	302.1968†	▼ 0.23	▲ 4.77	▼ 0.17	▲ 3.63	0.82	< 0.001
	5.14	324.1789*	▼ 0.26	▲ 4.73	▼ 0.11	▲ 3.65	0.72	< 0.001
	5.14	265.1052*	▼ 0.17	▲ 4.21	▼ 0.23	▲ 3.53	0.81	< 0.001
Car C10:2-OH	7.67	328.2125†	▼ 0.46	▲ 2.93	▼ 0.34	▲ 2.63	0.88	< 0.001
Car C11:2-OH	7.45	342.2277†	▼ 0.34	▲ 1.87	▼ 0.25	▲ 2.50	0.80	< 0.001
	7.47	305.1362*	▼ 0.35	▲ 1.85	▼ 0.14	▲ 2.19	0.76	< 0.001
Car C11:1-OH	7.75	344.2437†	▼ 0.30	▲ 1.97	▼ 0.15	▲ 2.45	0.81	< 0.001
	7.75	307.1513*	▼ 0.32	▲ 1.88	▼ 0.12	▲ 2.21	0.82	< 0.001
6β-OH Cortisol	7.01	379.2121†	▼ 0.05	▲ 3.62	▼ 0.03	▲ 2.85	0.82	< 0.001
	6.99	417.1879*	▼ 0.10	▲ 3.14	▼ 0.09	▲ 2.05	0.83	< 0.001
	7.01	401.1938*	▼ 0.16	▲ 4.54	▼ 0.11	▲ 3.00	0.84	< 0.001
	7.01	347.1846*	▼ 0.16	▲ 5.78	▼ 0.11	▲ 4.80	0.75	< 0.001
	7.01	423.2007*	▼ 0.17	▲ 5.73	▼ 0.11	▲ 4.54	0.74	< 0.001
16α-OH T sul	8.78	383.1525‡	▼ 0.46	▲ 3.17	▼ 0.13	▲ 2.63	0.83	< 0.001
	8.77	451.1397*	▼ 0.34	▲ 3.17	▼ 0.06	▲ 2.72	0.83	< 0.001
16α-OH An sul	8.39	385.1679‡	▼ 0.59	▲ 2.61	▼ 0.35	▲ 2.38	0.76	< 0.001
	8.41	453.1596*	▼ 0.55	▲ 2.19	▼ 0.20	▲ 2.03	0.83	< 0.001

Data are presented as fold-change *versus* control phase; increased with statistical significance (▲P <0.001, ▲P < 0.05) in the induction phase, decreased with statistical significance (▼P <0.001, ▼P <0.05) in the inhibition phase.

†, adduct form of $[M+H]^+$; ‡, adduct form of $[M-H]^-$; *, metabolic features that have same retention time and MS fragmentation pattern, so that considered as different adduct form or fragment of major metabolic feature (i.e. † or ‡).

Structure identification of novel CYP3A biomarkers

Five markers were identified as acylcarnitines, which had a peak of *m/z* 85 in positive ion mode and matched chemical formulas with the highest scores for MassLynx elemental composition (**Figure 3**). The potential position of the double bond for hydroxy octenoylcarnitine (Car C8:1-OH), hydroxy decadienoylcarnitine (Car C10:2-OH), hydroxy undecadienoylcarnitine (Car C11:2-OH), and hydroxy undecenoylcarnitine (Car C11:1-OH) was estimated from the MS/MS pattern of urinary acylcarnitine and related saturated acylcarnitine standard (**Figures 4-6**). Urinary 6β-OH cortisol was identified based on comparison of the MS/MS spectrum with authentic compounds (**Figure 7**). 16α-hydroxy testosterone sulfate (16α-OH TS) and 16α-hydroxy androsterone sulfate (16α-OH AS) were identified as follows (**Figures 8 and 9**): (1) an MS/MS fragmentation pattern of sulfate conjugation (*m/z* 96 in negative-ion mode) was present in blank urine; (2) the peak area of the sulfated metabolite decreased, and a desulfated metabolite peak arose in deconjugated urine that was not present in blank urine; and (3) the urinary deconjugated metabolite and authentic compound (16α-hydroxy testosterone; 16α-OH T or 16α-hydroxy androsterone; 16α-OH A) had identical MS/MS patterns.

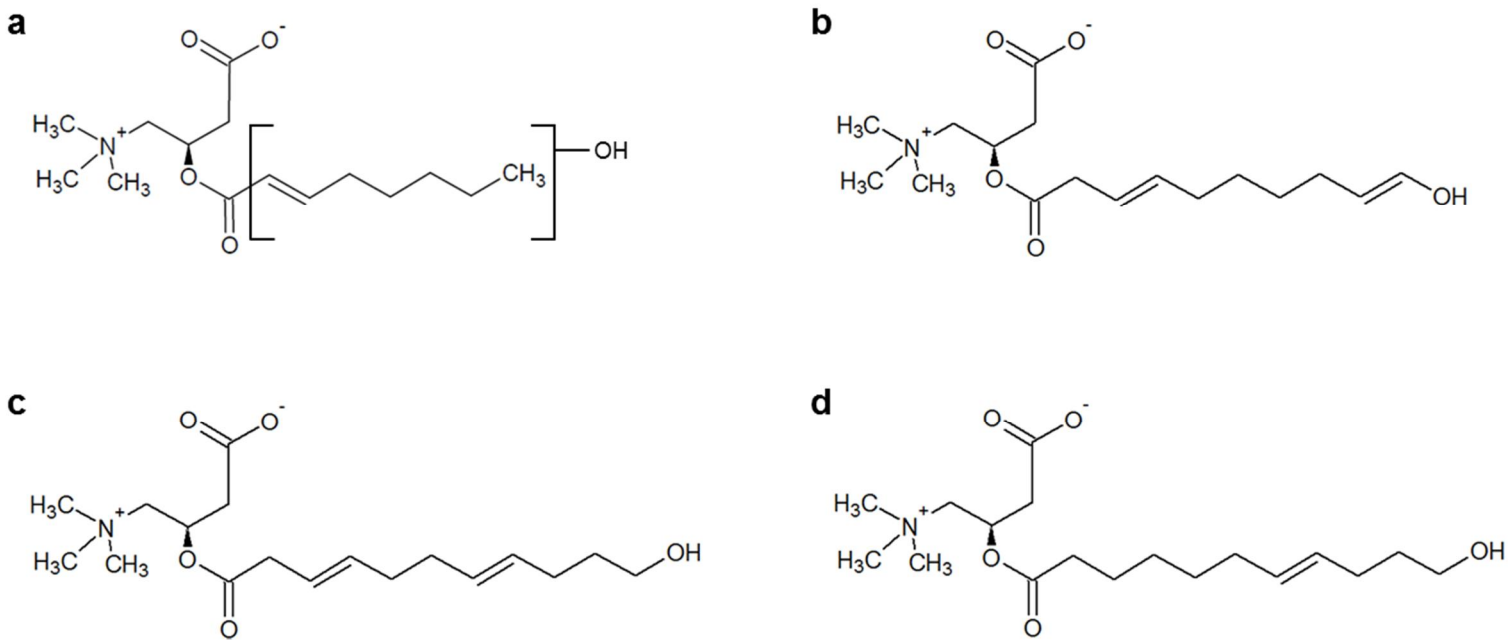

Figure 3. Structures of the identified urinary acylcarnitines; (a) Car C8:1-OH I and II, (b) Car C10:2-OH, (c) Car C11:2-OH, and (d) Car C11:1-OH.

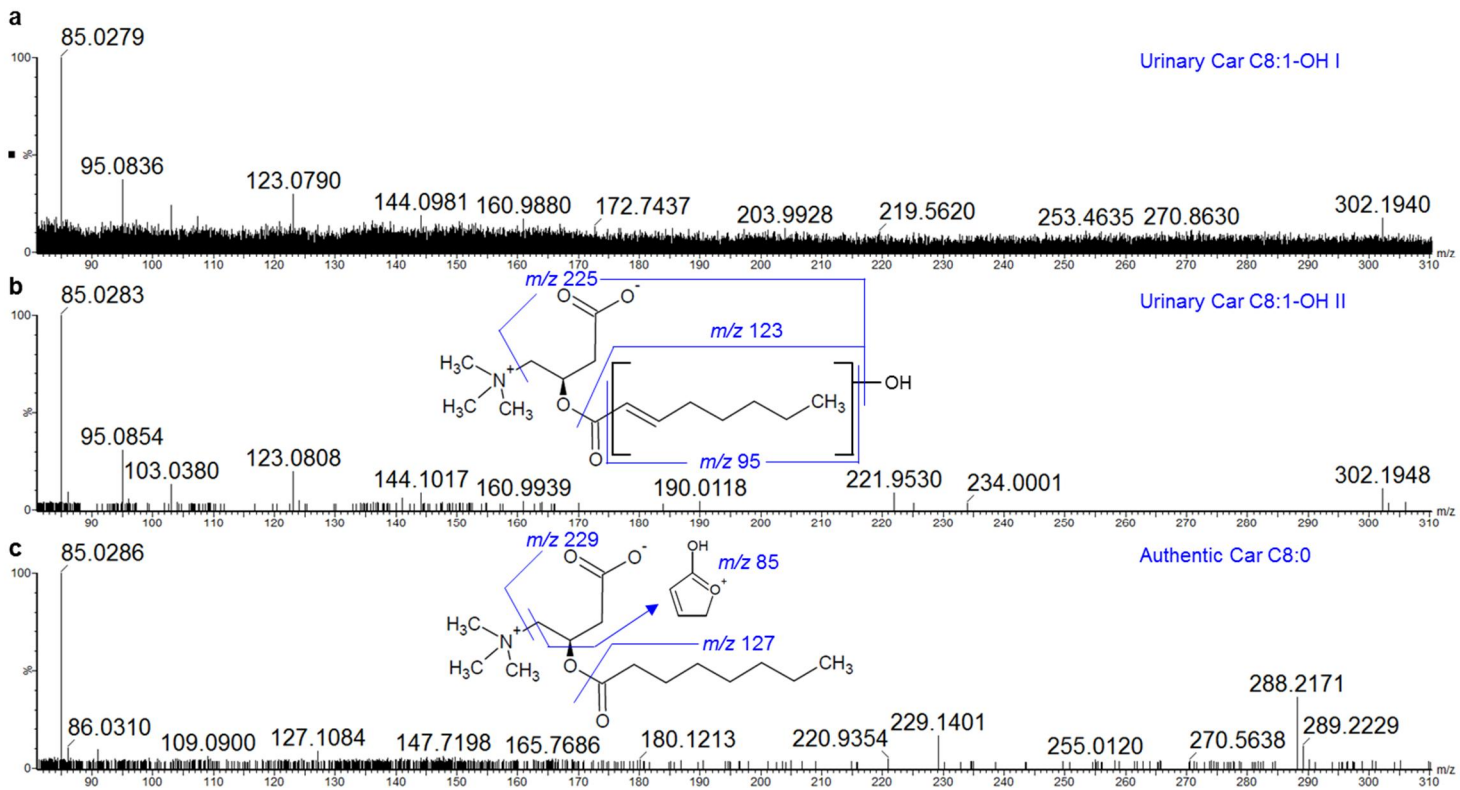

Figure 4. Identification and characterization of Car C8:1-OH. MS/MS spectra of (a) urinary Car C8:1-OH I, (b) urinary C8:1-OH II, and (c) authentic Car C8:0.

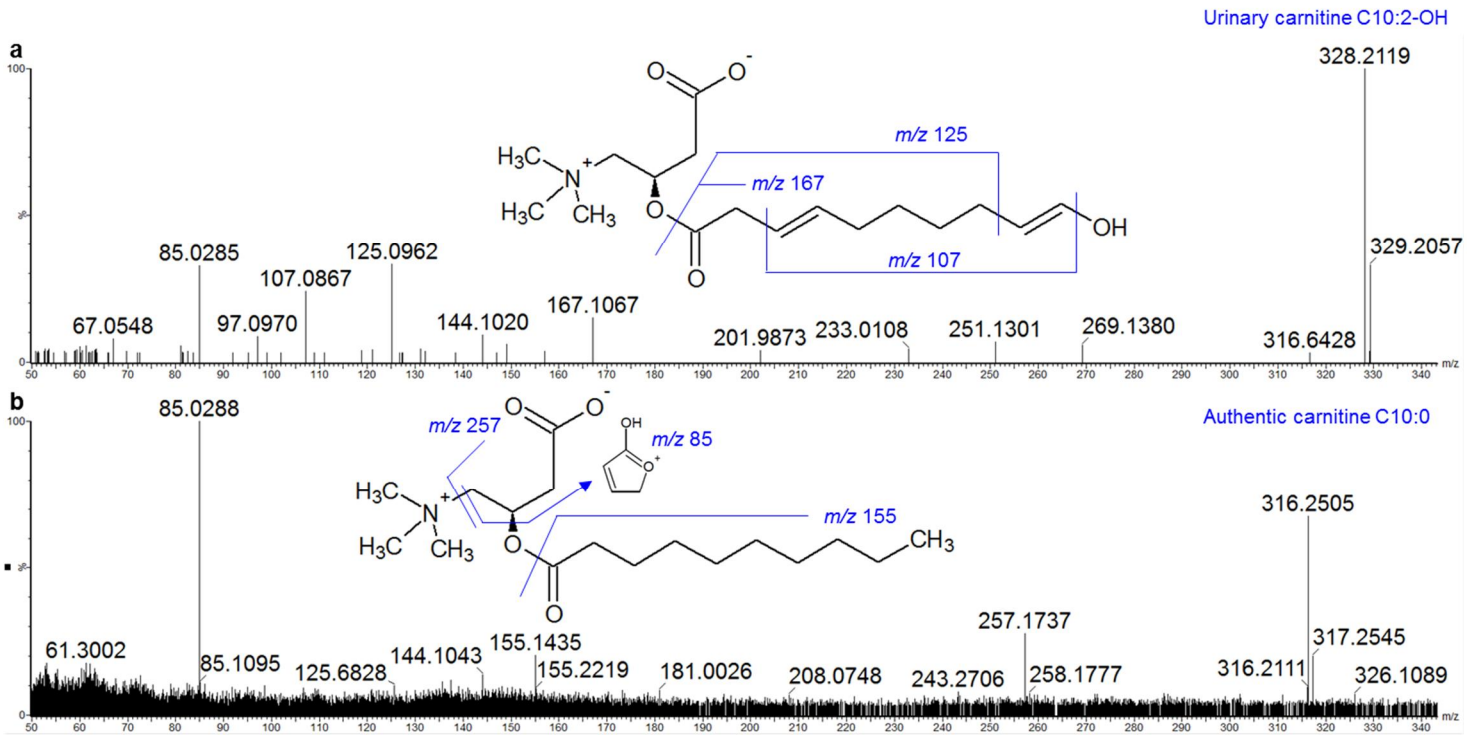

Figure 5. Identification and characterization of Car C10:2-OH. MS/MS spectra of (a) urinary Car C10:2-OH, and (b) authentic Car C10:0.

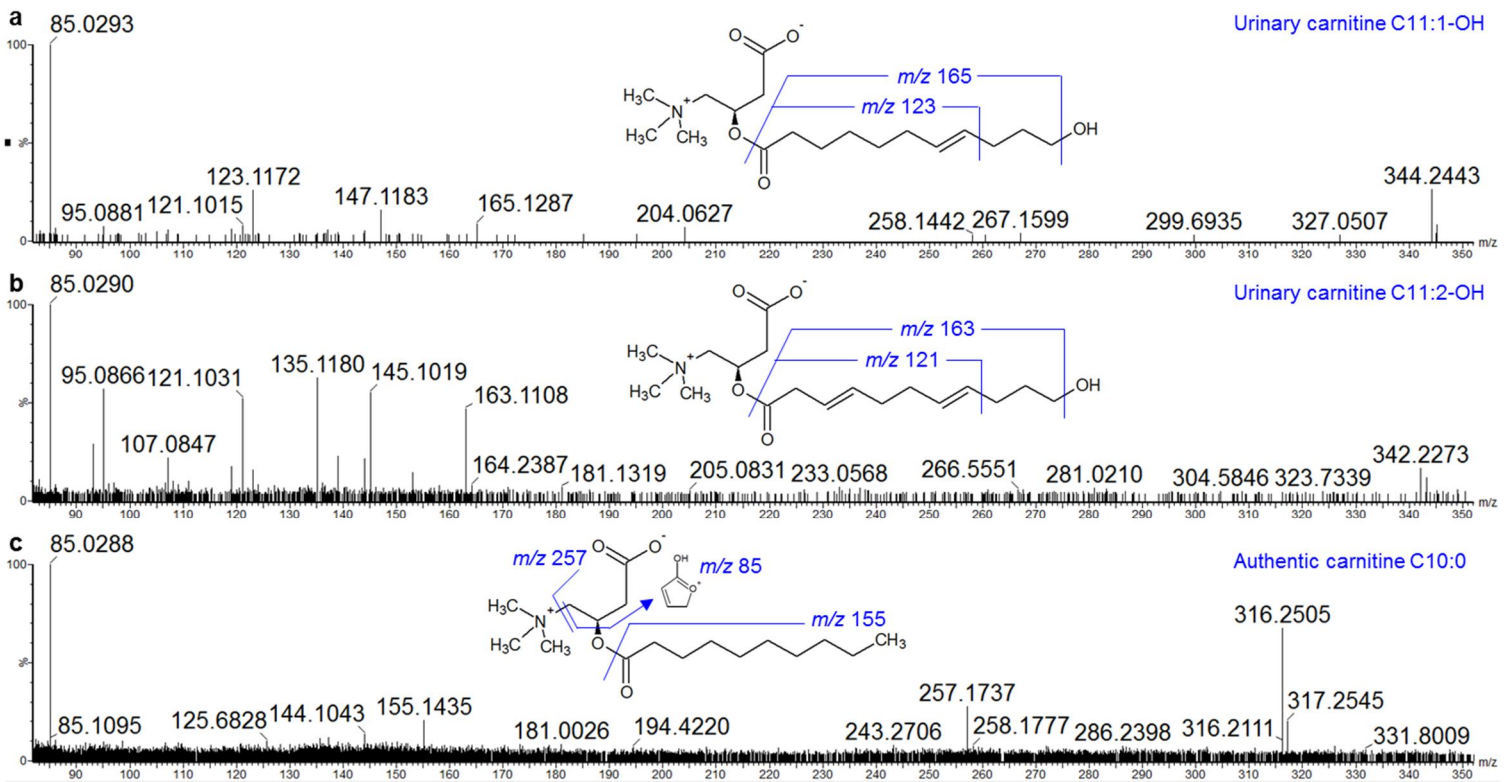

Figure 6. Identification and characterization of Car C11:2-OH and Car C11:1-OH. MS/MS spectra of (a) urinary Car C11:1-OH, (b) urinary C11:2-OH, and (c) authentic Car C10:0.

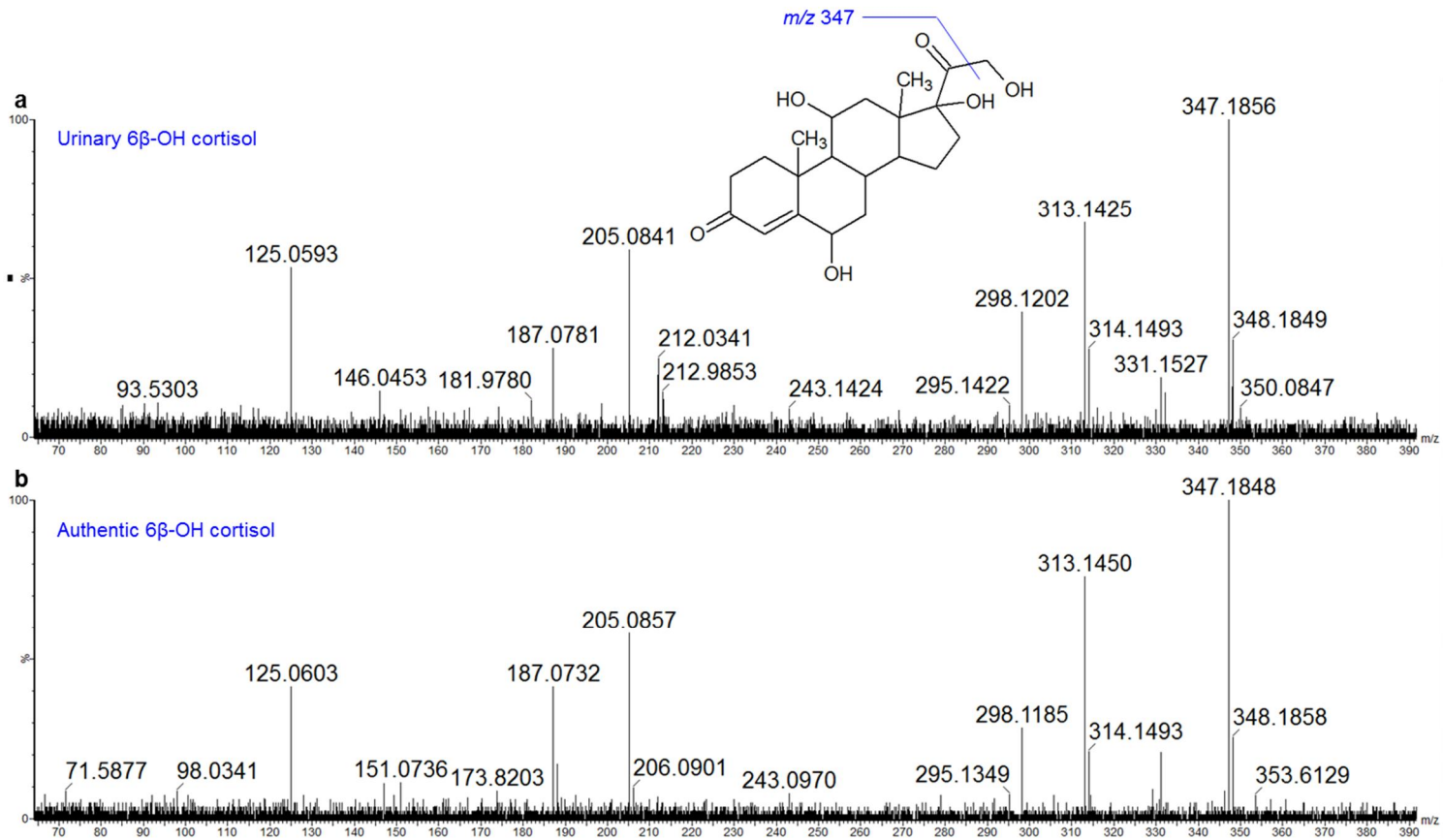

Figure 7. Identification and characterization of 6β-OH cortisol. MS/MS spectra of (a) urinary 6β-OH cortisol and (b) authentic 6β-OH cortisol.

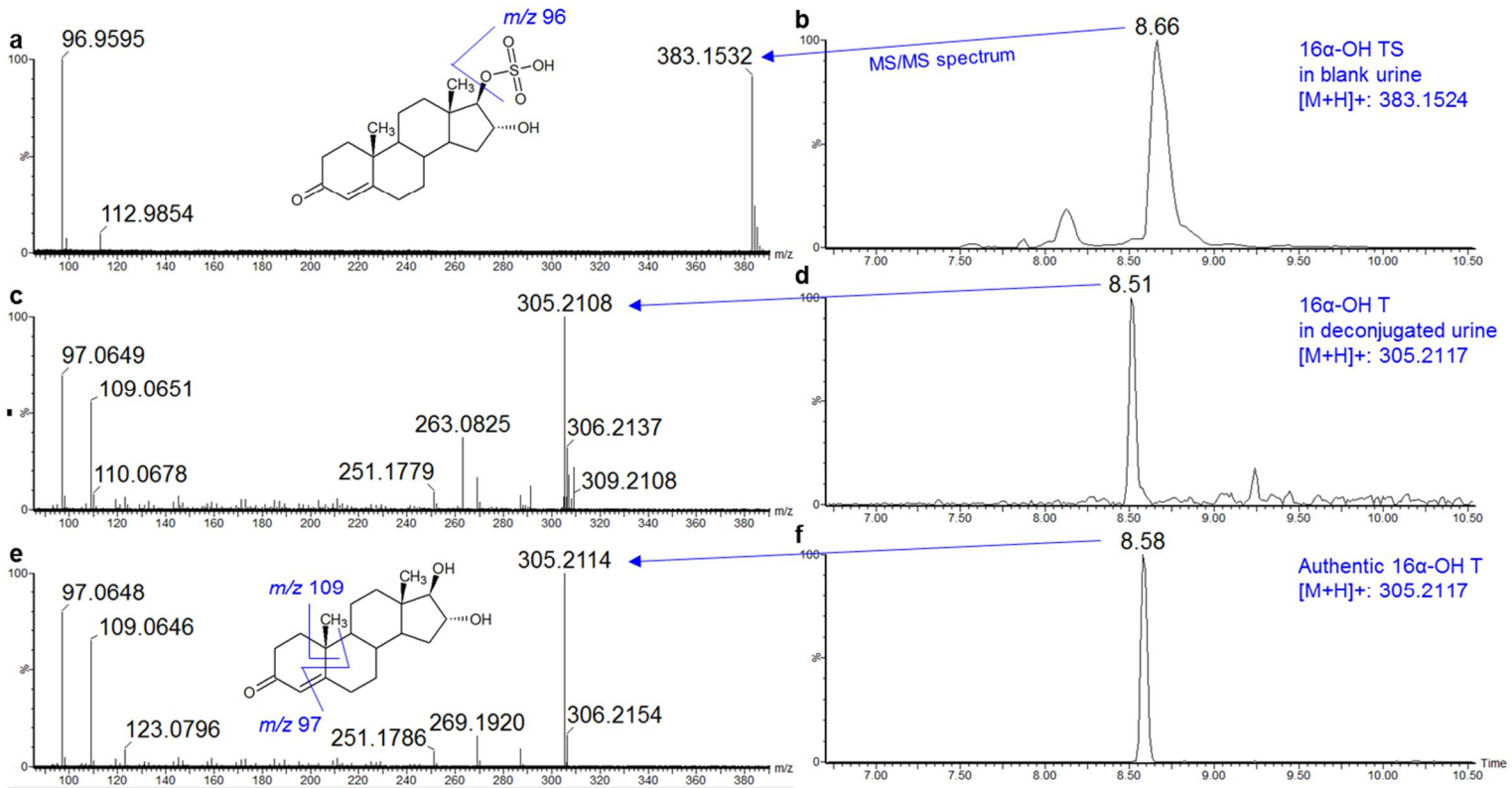

Figure 8. Identification and characterization of 16α-OH TS. MS/MS spectra and chromatograms of (a, b) urinary 16α-OH TS, (c, d) 16α-OH T in deconjugated urine and (e, f) authentic 16α-OH TS.

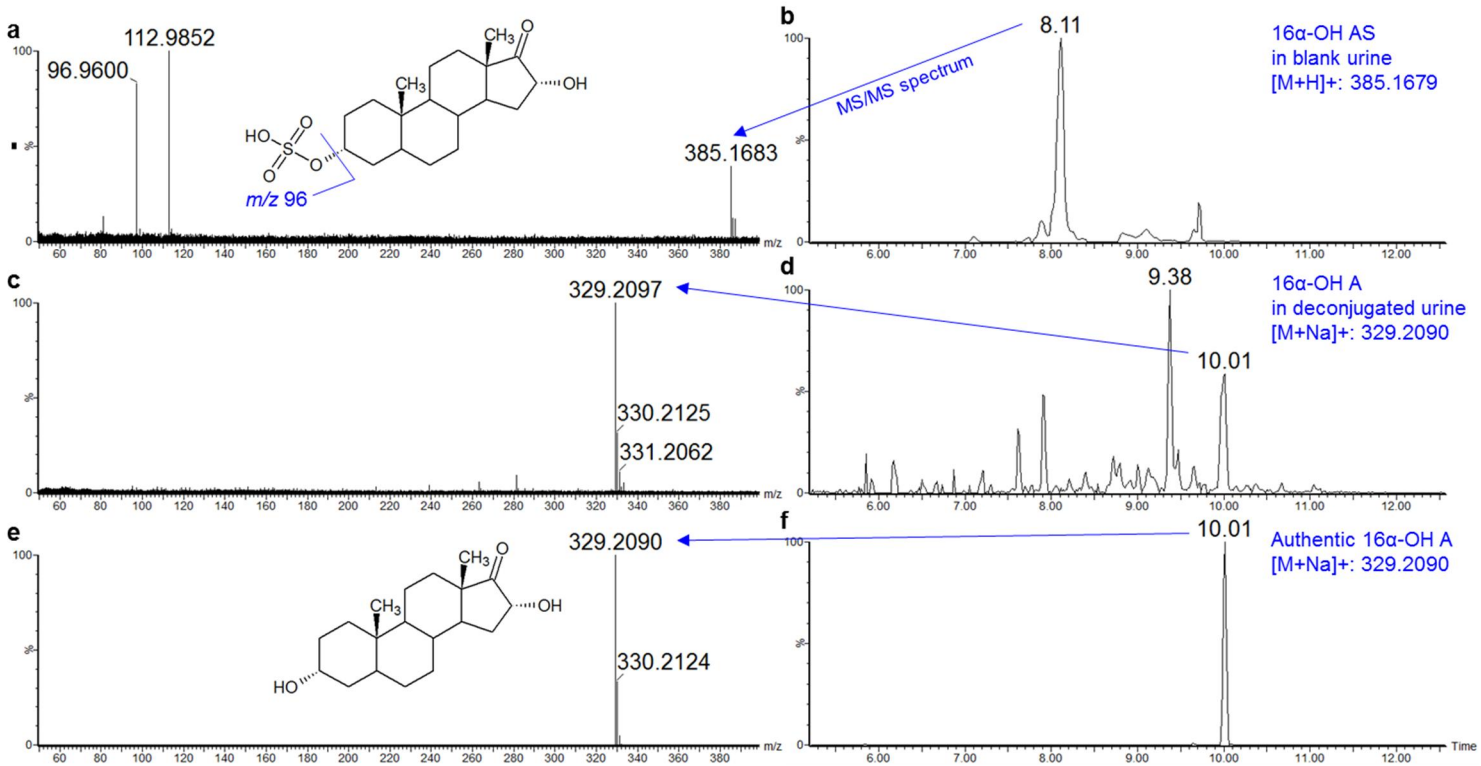

Figure 9. Identification and characterization of 16α-OH AS. MS/MS spectra and chromatograms of (a, b) urinary 16α-OH AS, (c, d) 16α-OH A in deconjugated urine and (e, f) authentic 16α-OH AS.

ω- and (ω-1)-hydroxylations of octenoic acid by CYP3A4

All acylcarnitine markers included a hydroxylated unsaturated medium-chain fatty acid (MCFA, C8-C12); aliphatic hydroxylation is a major metabolic reaction of CYP3A4. To identify the regioselectivity of MCFA hydroxylation by CYP3A4, C8 fatty acids (octanoic, 2-octenoic, 3-octenoic, and 7-octenoic acids) were incubated with CYP3A4 supersomes (**Figure 10**). The chromatograms of hydroxylated octanoic acid and octenoic acids indicated that 2- and 3-octenoic acid were hydroxylated, but octanoic acid and 7-octenoic acid were not hydroxylated by CYP3A4, suggesting that the saturated fatty acid is not hydroxylated but unsaturated fatty acids are ω- and (ω-1)-hydroxylated by CYP3A4 (**Figure 10a-10d**). The 4 hydroxylated octenoic acids (peaks I-IV in **Figures 10b and 10c**) were not compared with authentic hydroxy octenoic acids because these are not commercially available; however, terminally ω-hydroxylated fatty acids tended showed lower column retention than front end-hydroxylated fatty acids (**Figure 11**). Thus, peaks I and III were identified as ω-hydroxylated octenoic acid, while peaks II and IV were identified as (ω-1)-hydroxylated octenoic acid. The MS/MS spectra of hydroxylated 2- and 3-octenoic acids were similar to that of authentic 8-hydroxy octanoic acid (**Figure 10e-10i**). To confirm the regioselective ω- and (ω-1)-hydroxylation activity of CYP3A4, we compared the peaks of hydroxylated octenoic acid upon incubation with CYP3A4 supersomes with those of ω- and (ω-1)-hydroxylated octenoic acid upon incubation with CYP4A11 or CYP4F2, which catalyze the ω- and (ω-1)-hydroxylation of saturated, branched-chain, and unsaturated fatty acids [24] (**Figure 12**). No differences in peak retention time were observed; thus, CYP3A4 is regioselective for ω- and (ω-1)-hydroxylation.

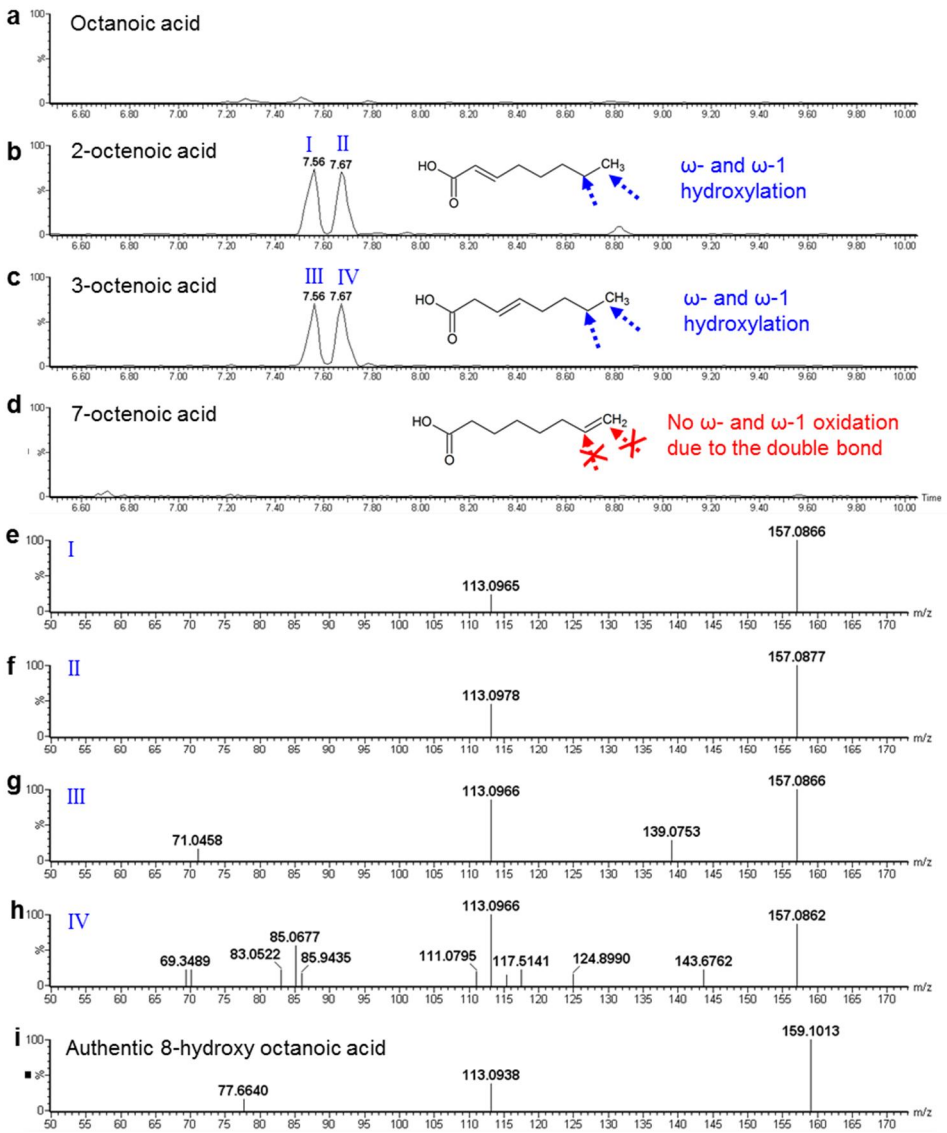

Figure 10. Identification of ω- and (ω-1)-hydroxylation of C8 fatty acids by CYP3A4. Chromatogram of hydroxylated (a) octanoic acid, (b) 2-octenoic acid, (c) 3-octenoic acid and (d) 7-octenoic acid by incubation in CYP3A4 supersomes. MS/MS spectrum of ω- (I and III) and (ω-1)- (II and IV) hydroxylated (e, f) 2-octenoic acid and (g, h) 3-octenoic acid by CYP3A4 supersome incubation. MS/MS spectrum of (i) authentic 8-hydroxy octanoic acid.

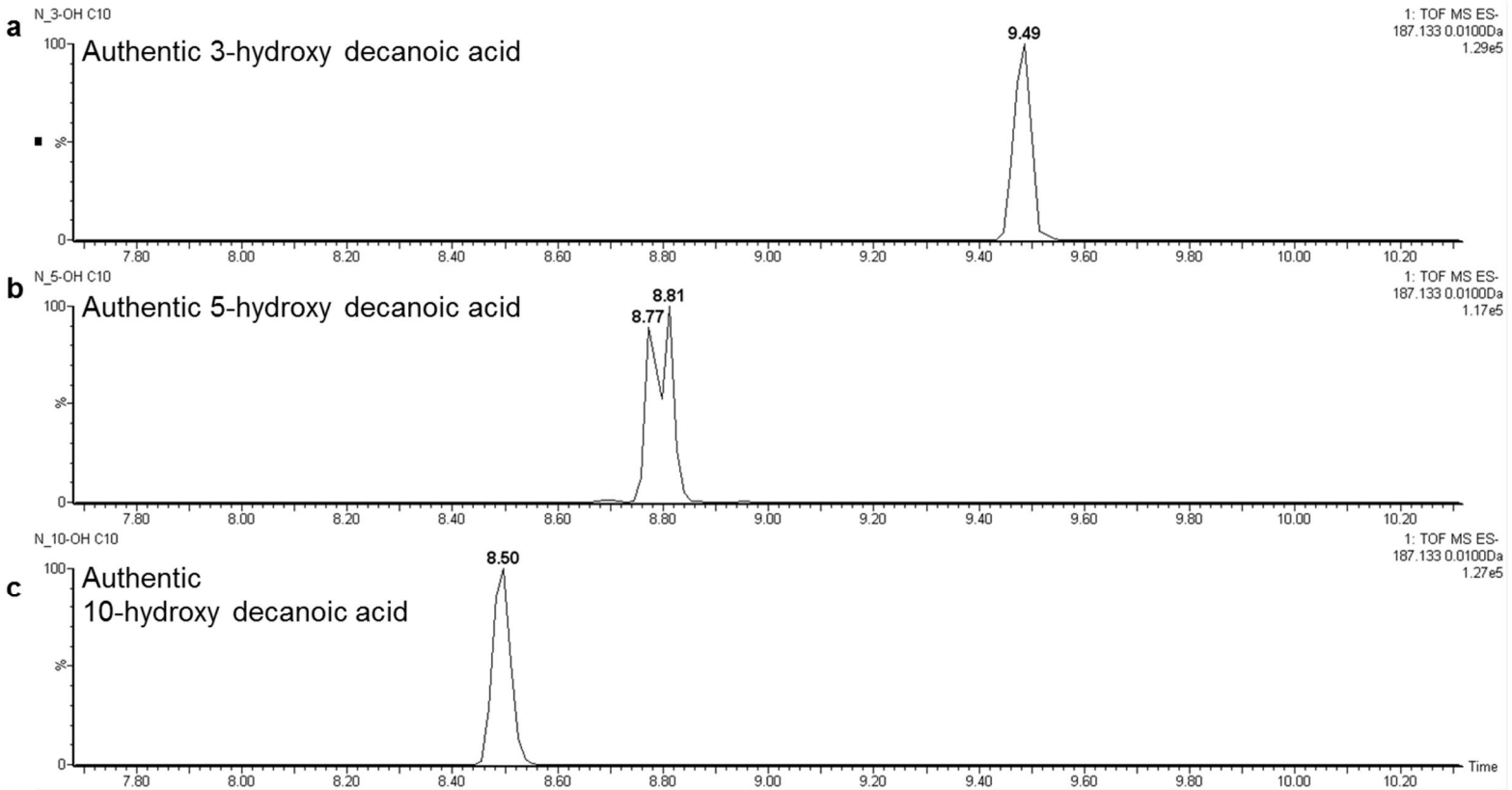

Figure 11. Chromatogram of authentic (a) 3-hydroxy decanoic acid, (b) 5-hydroxy decanoic acid, (c) 10-hydroxy decanoic acid.

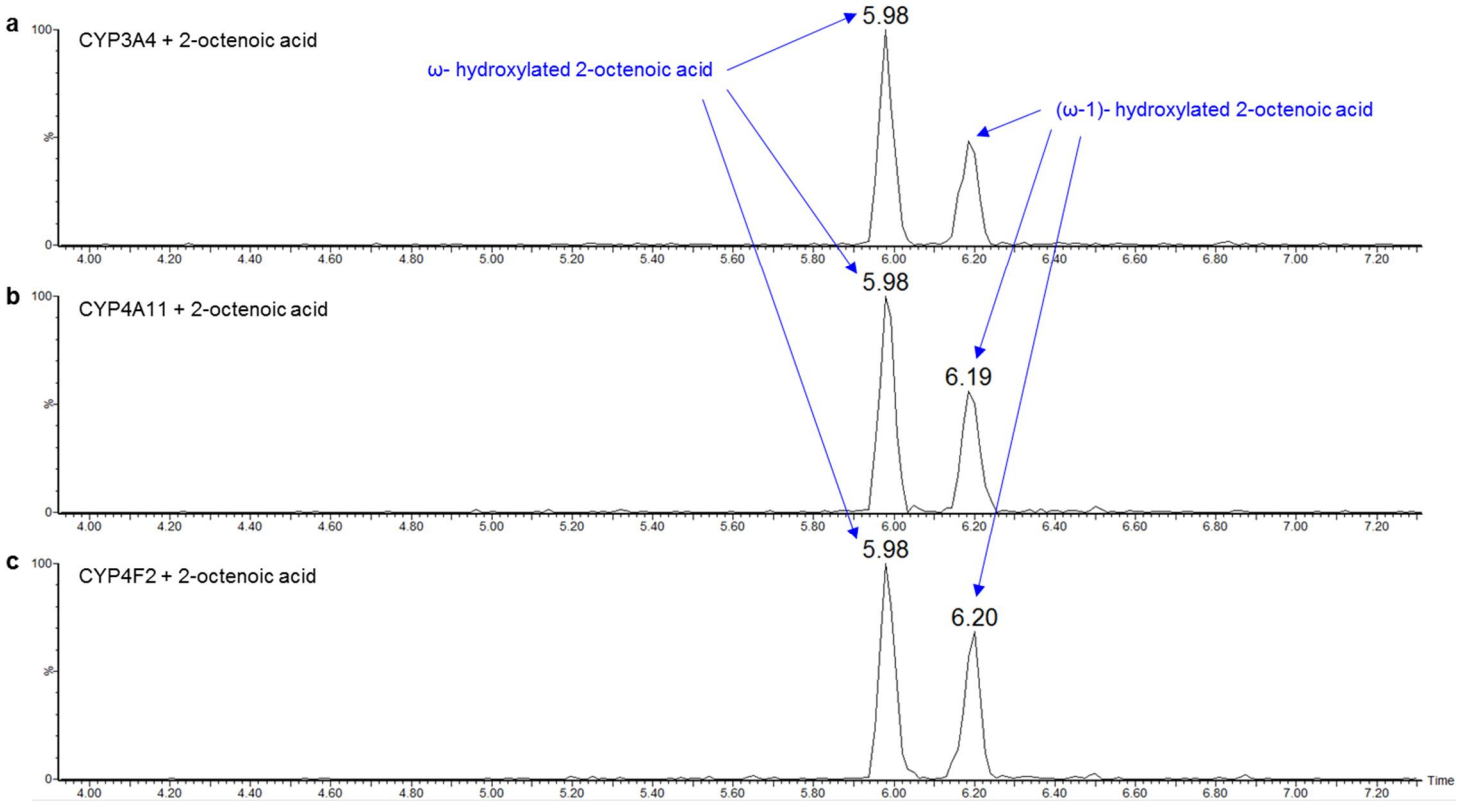

Figure 12. Confirmation of ω- and (ω-1)-hydroxylation of 2-octenoic acid by CYP3A4. Chromatogram of hydroxylated 2-octenoic acid by (a) CYP3A4, (b) CYP4A11, (c) CYP4F2.

Kinetic parameters of ω- and (ω-1)-hydroxylation by CYP3A4, CYP4A11, and CYP4F2

The kinetics of ω- and (ω-1)-hydroxylation of 2-octenoic acid by CYP3A4, CYP4A11, and CYP4F2 were further investigated using recombinantly expressed enzymes and non-linear regression analysis using a Michaelis-Menten model (**Figure 13a and 13b**). To illustrate kinetic parameters of 2-octenoic acid ω- and (ω-1)-hydroxylation, Lineweaver-Burk plots for ω- and (ω-1)-hydroxlyation of 2-octenoic acid (1/[2-octenoic acid], range, 0.1 to 2.0) are shown in **Figure 13c and 13d**. All three enzymes catalyzed the formation of ω- and (ω-1)-hydroxy-2-octenoic acid, with CYP3A4 being the most efficient and with the lowest Km values of 1.43 mM and 2.99 mM, respectively, and the highest Vmax/Km ratios of 0.84 and 0.82, respectively (**Table 5**). Vmax/Km of ω-hydroxylation was similar for CYP4A11 (0.44) and CYP4F2 (0.52), while it was ~2-fold higher for CYP3A4 (0.84). For (ω-1)-hydroxylation, CYP3A4 (Vmax/Km of 0.82) was followed by CYP4A11 (Vmax/Km of 0.59) and CYP4F2 (Vmax/km of 0.50).

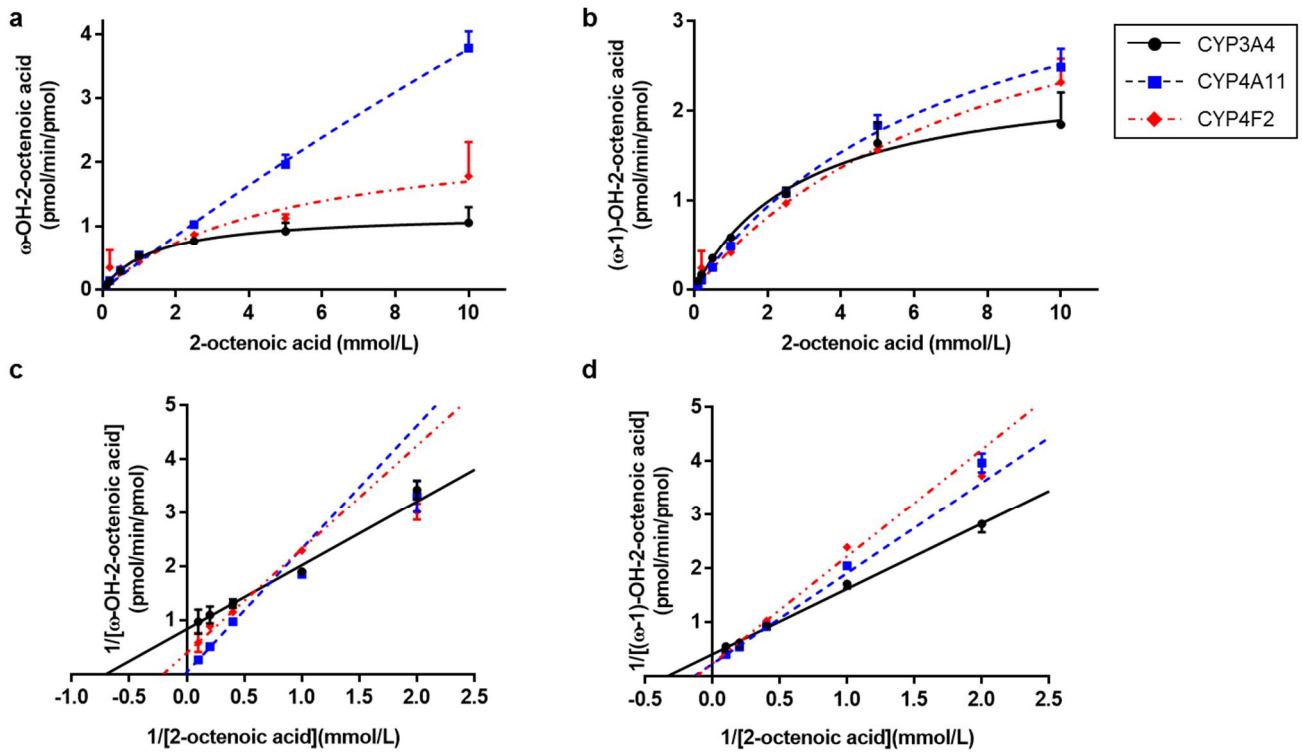

Figure 13. Michaelis-Menten model for 2-octenoic acid (a) ω- and (b) (ω-1)-hydroxylation by CYP3A4, CYP4A11, or CYP4F2 supersomes. Lineweaver-Burk plots of (c) ω- and (d) (ω-1)-hydroxylation of 2-octenoic acid by CYP3A4, CYP4A11, or CYP4F2 supersomes. Each point represents the mean of duplicate determinations.

Table 5. Kinetic parameters for ω- and (ω-1)-hydroxylation of 2-octenoic acid by CYP3A4, CYP4A11, and CYP4F2

Enzyme	Km (mM)		Vmax (pmol/min/pmol P450)		Vmax/Km	
	ω	ω-1	ω	ω-1	ω	ω-1
CYP3A4	1.43±0.78	2.99±1.50	1.20±0.32	2.46±0.76	0.84	0.82
CYP4A11	64.22±10.58	7.34±1.09	27.96±6.00	4.36±0.64	0.44	0.59
CYP4F2	4.89±5.16	8.52±3.16	2.53±1.69	4.28±1.20	0.52	0.5

Values of Km and Vmax are presented as mean ± SD

Inhibitory effect of ketoconazole on CYP3A4, CYP4A11, and CYP4F2

To determine whether ketoconazole inhibits CYP4F2 and/or CYP4A11, ketoconazole, a known CYP3A-specific inhibitor, was incubated with 2-octenoic acid (2.5 mM) with CYP3A4, CYP4A11, or CYP4F2 recombinant enzymes (**Figure 14**). Ketoconazole inhibited the formation of ω- and (ω-1)-hydroxy-2-octenoic acid by CYP3A4 with half-maximal inhibitory concentration (IC_{50}) values of 213.9 μM and 41.6 μM, respectively, and maximum inhibition of 27–40%. However, ketoconazole decreased the ω- and (ω-1)-hydroxylation of 2-octenoic acid by CYP4A11 and CYP4F2 by 5–14%, suggesting that it exerts only weak or no inhibitory action on CYP4 enzymes.

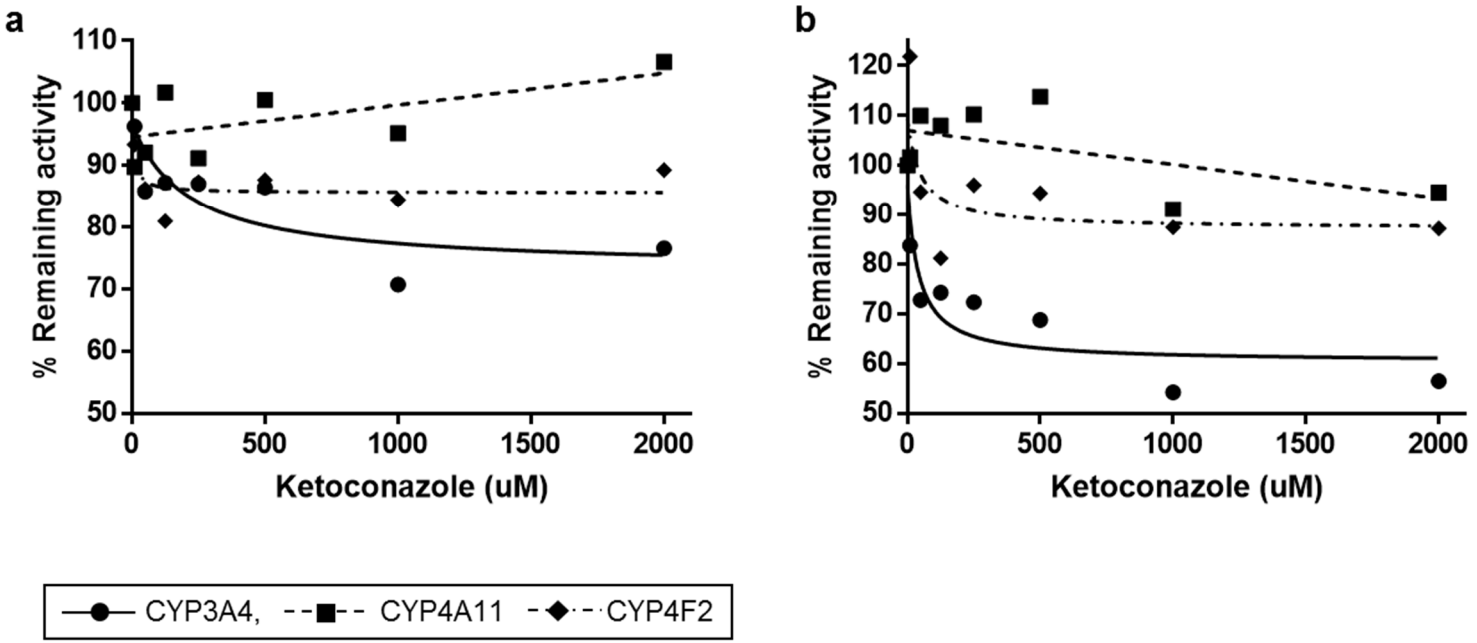

Figure 14. Inhibition of 2-octenoic acid (2.5 mM) (a) ω- and (b) (ω-1)-hydroxylation by ketoconazole in CYP3A4, CYP4A11, or CYP4F2 supersomes. The percentage of 2-octenoic acid (a) ω- and (b) (ω-1)-hydroxylation activity remaining in each supersome relative to control was determined in the presence of ketoconazole.

Metabolic marker changes by CYP3A activity states

Eight endogenous urinary metabolites significantly associated with CYP3A activity were (semi-)quantitated and normalized to creatinine (Cr) concentration in each phase. **Figure 15** shows the significant elevations in urinary concentrations of the 8 metabolites in accordance with increased CYP3A activity. The individual changes in urinary concentrations of 8 metabolites that were observed in the inhibition, control, and induction phase are presented in **Figure 16-23**. Fold-changes over the control phase are listed in **Table 6**. Except for Car C8:1-OH I in the inhibition phase, all metabolites were significantly reduced and increased in the inhibition and induction phase, respectively, as compared to the control phase. The largest increases were observed for Car C8:1-OH I (13.16-fold in males and 7.91-fold in females) and Car C8:1-OH II (6.11-fold in males and 6.21-fold in females). 6β-OH cortisol and Car C8:1-OH II demonstrated the greatest decreases (<0.2-fold changes in both males and females) in the inhibition phase.

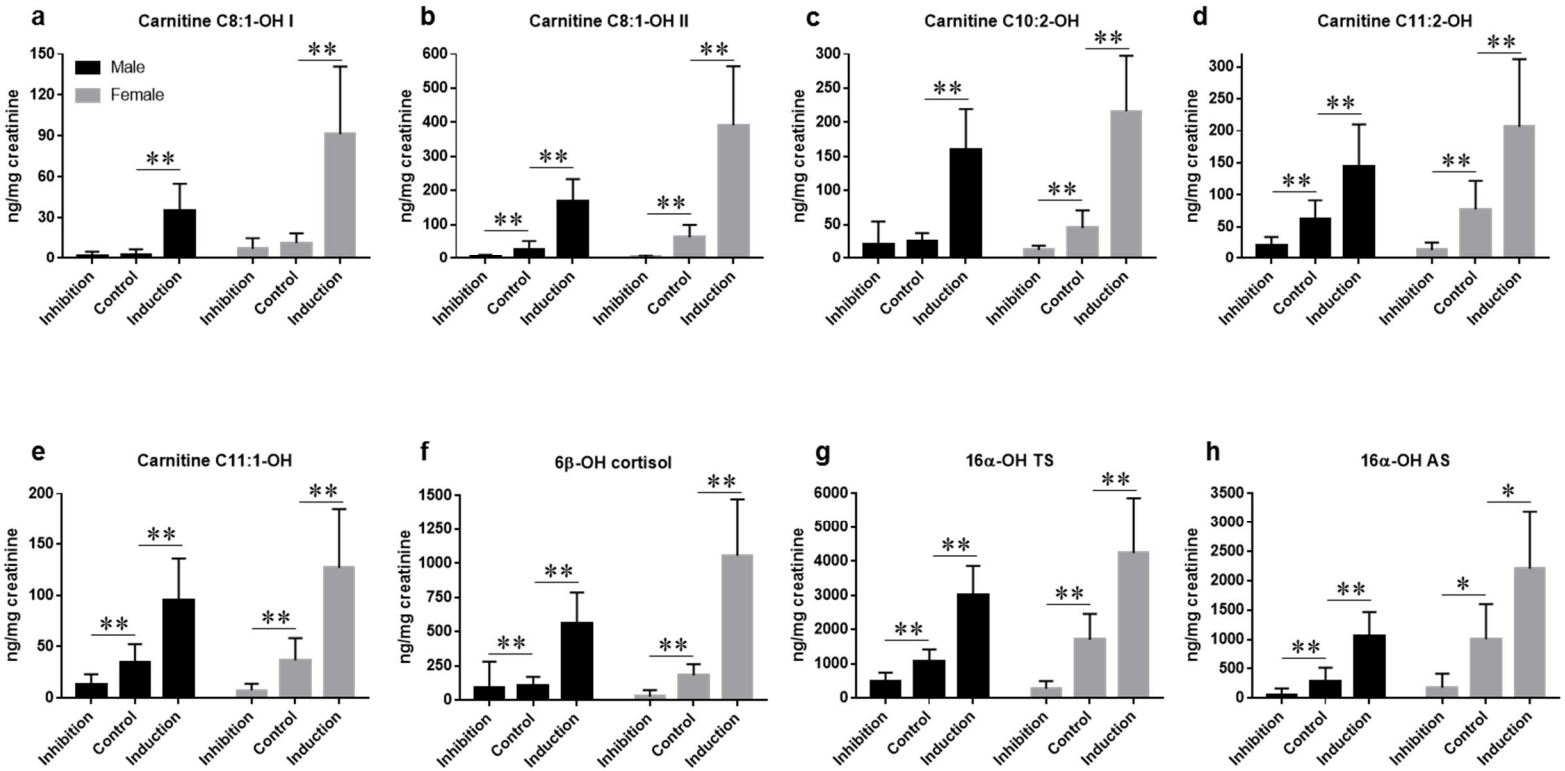

Figure 15. Concentrations (mean ± SD) of urinary CYP3A markers of (a) Car C8:1-OH I/Cr, (b) Car C8:1-OH II/Cr, (c) Car C10:2-OH/Cr, (d) Car C11:2-OH/Cr, (e) Car C11:1-OH/Cr, (f) 6β-OH cortisol/Cr, (g) 16α-OH TS/Cr, and (h) 16α-OH AS/Cr in CYP3A inhibition, control, and induction phases. $^{**}P < 0.001$, $^{*}P < 0.05$ *versus* control groups of male (N = 24) and female (N = 12) subjects.

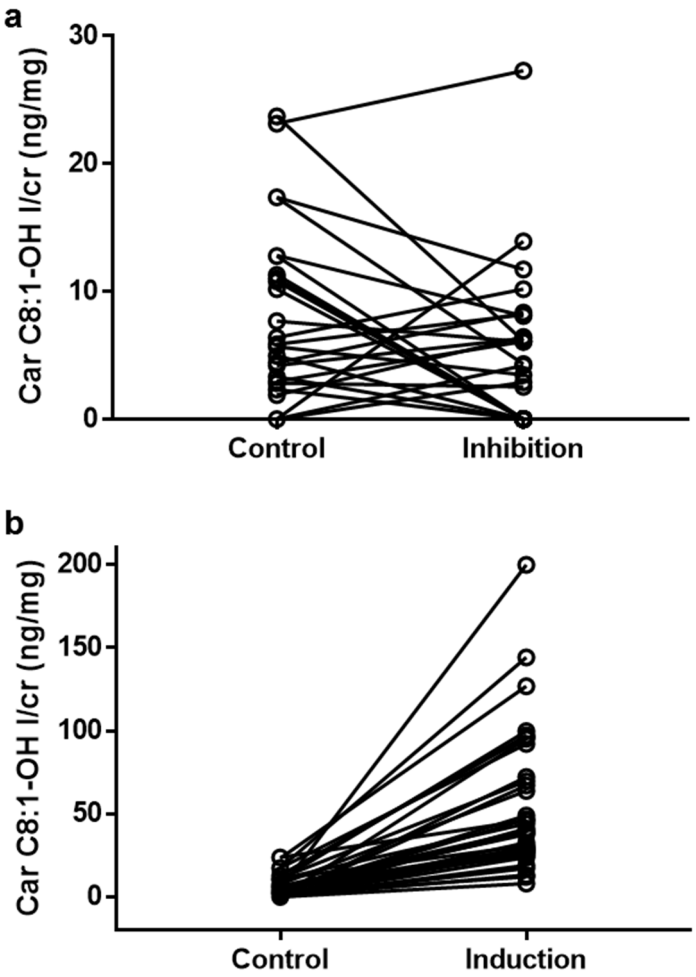

Figure 16. Individual Car C8:1-OH I/cr concentrations in (a) CYP3A- control and inhibition phases and (b) control and induction phases

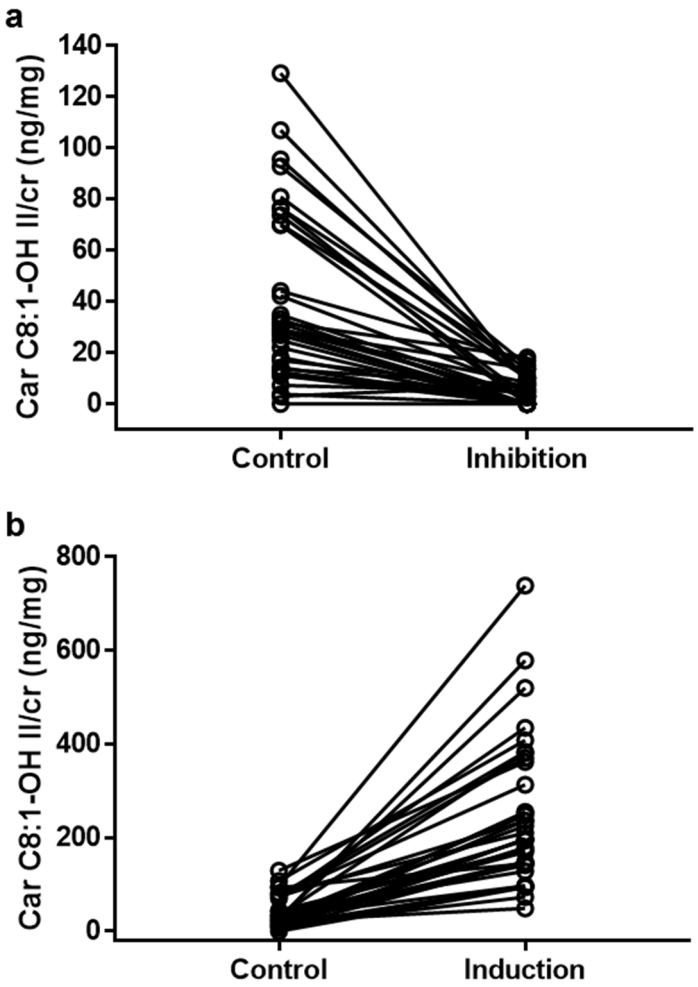

Figure 17. Individual Car C8:1-OH II/cr concentrations in (a) CYP3A-control and inhibition phases and (b) control and induction phases

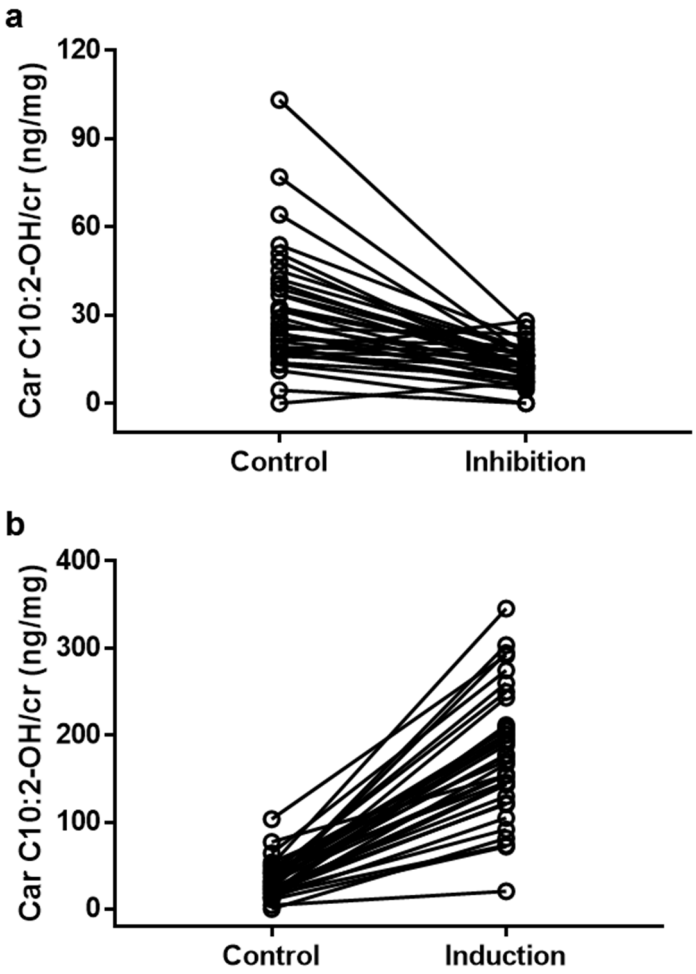

Figure 18. Individual Car C10:2-OH/cr concentrations in (a) CYP3A- control and inhibition phases and (b) control and induction phases

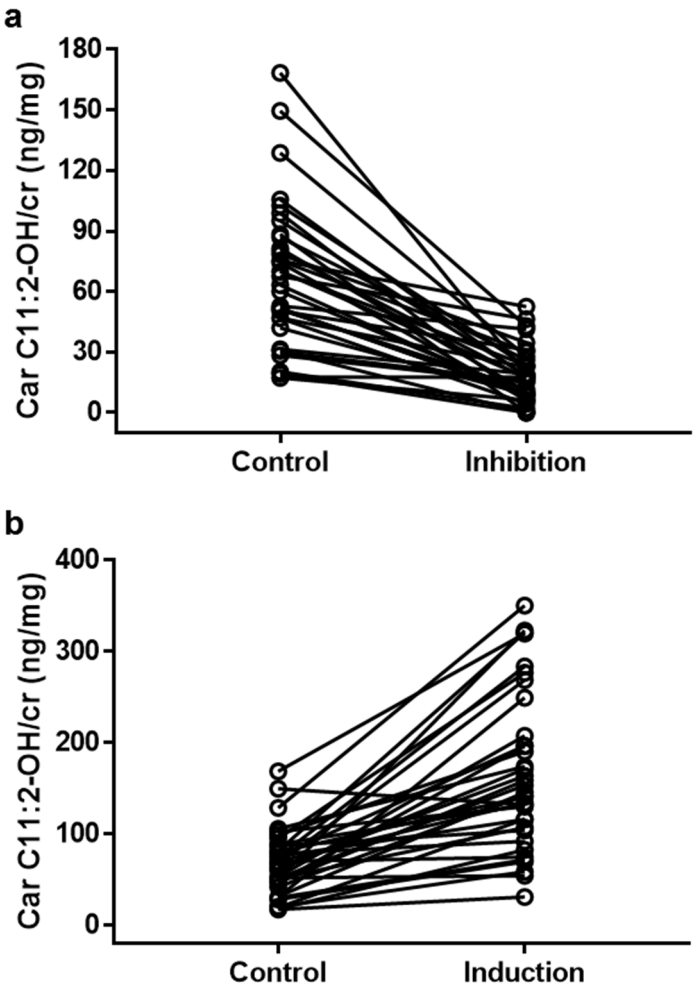

Figure 19. Individual Car C11:2-OH/cr concentrations in (a) CYP3A-control and inhibition phases and (b) control and induction phases

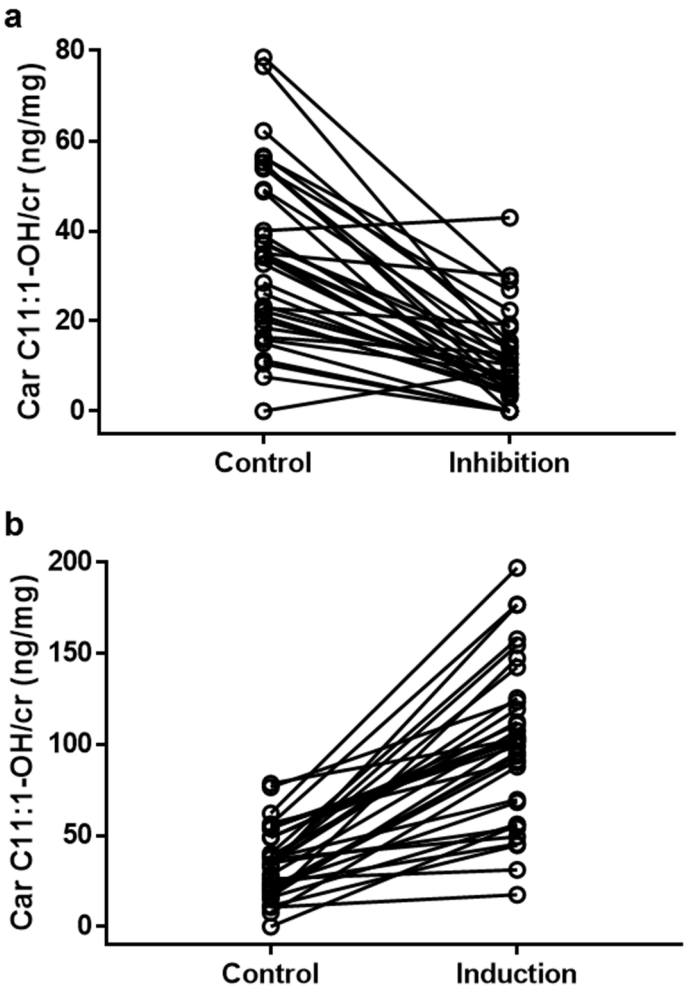

Figure 20. Individual Car C11:1-OH/cr concentrations in (a) CYP3A-control and inhibition phases and (b) control and induction phases

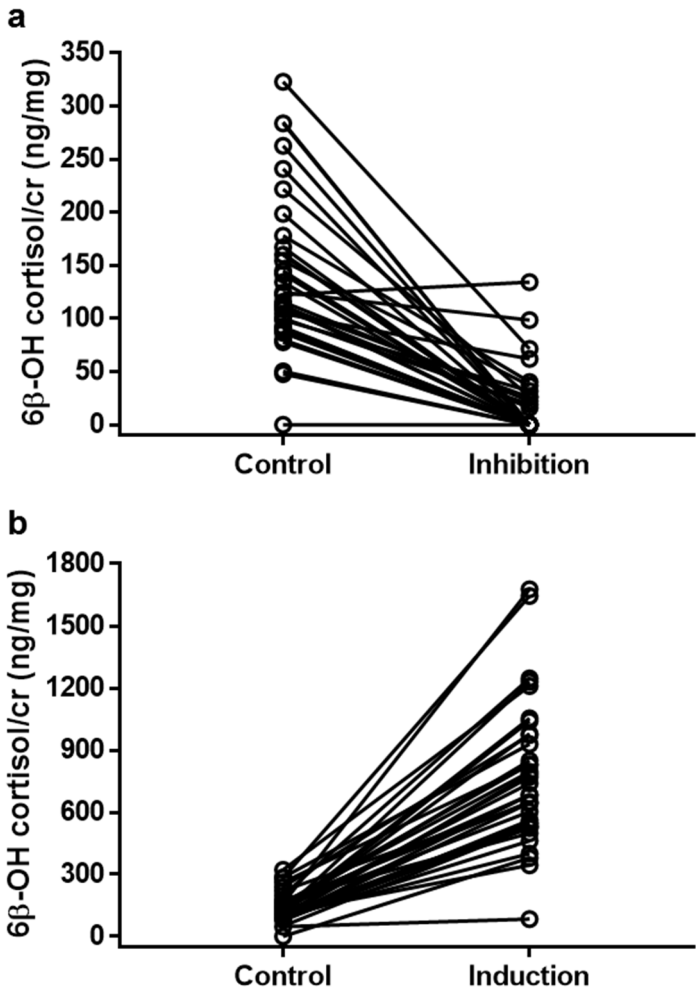

Figure 21. Individual 6β-OH cortisol/cr concentrations in (a) CYP3A-control and inhibition phases and (b) control and induction phases

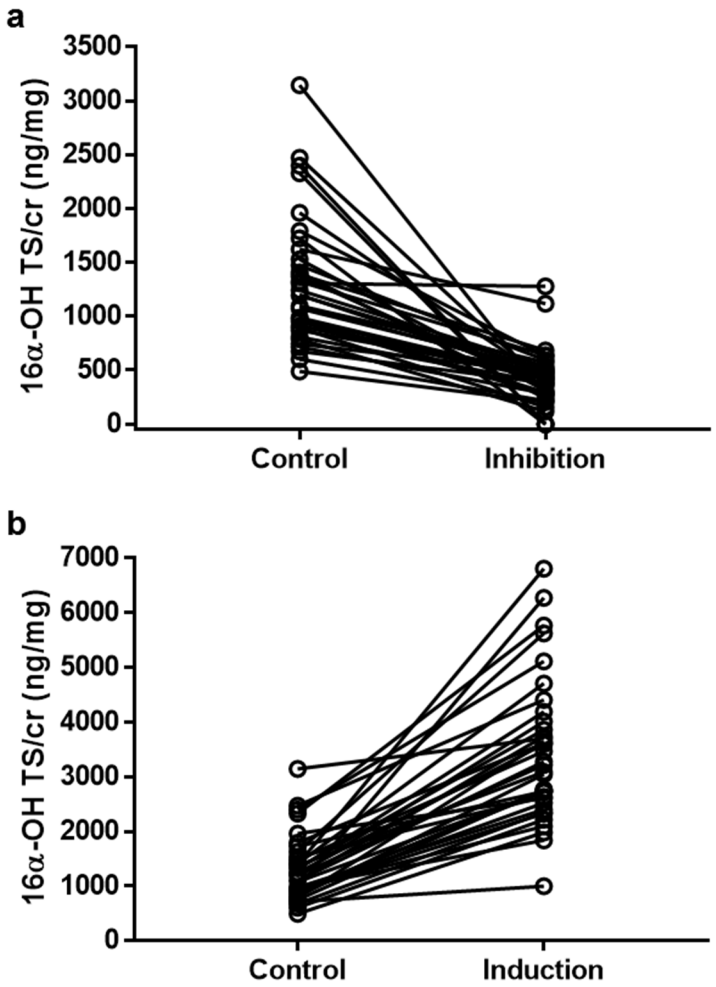

Figure 22. Individual 16α-OH TS/cr concentrations in (a) CYP3A-control and inhibition phases and (b) control and induction phases

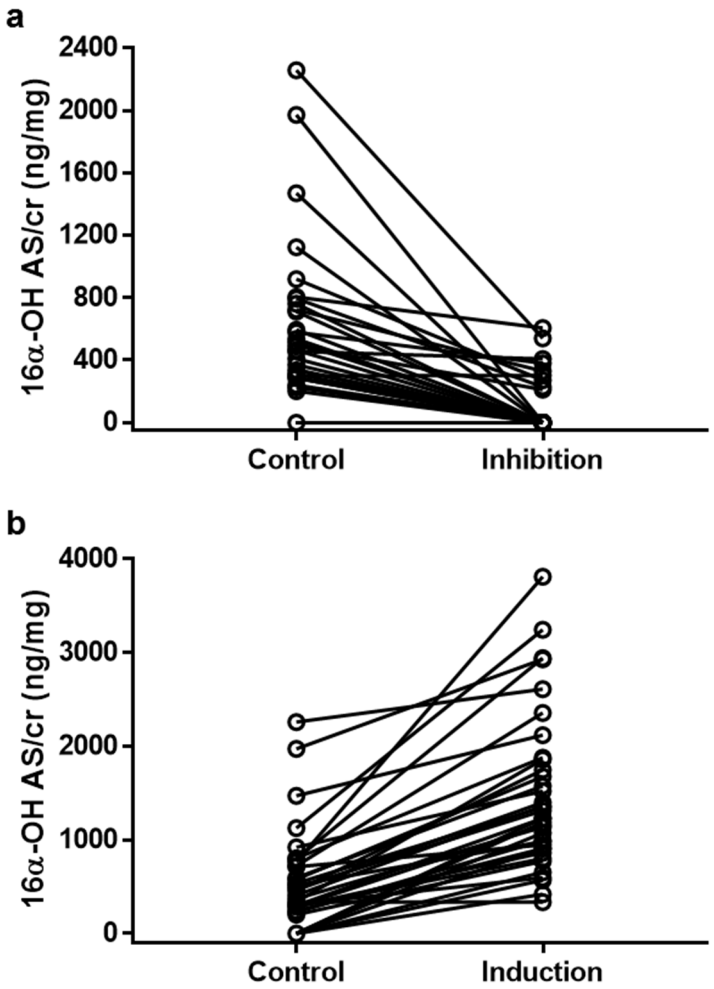

Figure 23. Individual 16α-OH AS/cr concentrations in (a) CYP3A-control and inhibition phases and (b) control and induction phases

Table 6. Identified urinary CYP3A biomarkers and their mean concentration fold-changes in CYP3A inhibition and induction phases as compared to the control phase, and correlation with midazolam clearance

Metabolites	RT (min)	Mass (*m/z*)	Fold-change in males		Fold-change in females		Correlation with midazolam clearance	
			Inhibition phase	Induction phase	Inhibition phase	Induction phase	r	*P*
Car C8:1-OH I	4.93	302.1962	0.81	▲ 13.16	0.63	▲ 7.91	0.608	< 0.001
Car C8:1-OH II	5.14	302.1968	▼ 0.19	▲ 6.11	▼ 0.07	▲ 6.21	0.788	< 0.001
Car C10:2-OH	7.67	328.2125	0.83	▲ 6.41	▼ 0.29	▲ 4.76	0.797	< 0.001
Car C11:2-OH	7.45	342.2277	▼ 0.33	▲ 2.33	▼ 0.18	▲ 2.68	0.801	< 0.001
Car C11:1-OH	7.75	344.2437	▼ 0.37	▲ 2.79	▼ 0.20	▲ 3.44	0.801	< 0.001
6β-OH cortisol	7.00	379.2121	▼ 0.10	▲ 5.18	▼ 0.14	▲ 5.82	0.772	< 0.001
16α-OH TS	8.78	383.1525	▼ 0.45	▲ 2.77	▼ 0.16	▲ 2.48	0.855	< 0.001
16α-OH AS	8.39	385.1679	▼ 0.17	▲ 3.74	▼ 0.18	▲ 2.21	0.493	< 0.001

Car C8:1-OH I, hydroxy octenoyl carnitine I; Car C8:1-OH II, hydroxy octenoyl carnitine II; Car C10:2-OH, hydroxy decadienoyl carnitine; Car C11:2-OH, hydroxy undecadienoyl carnitine; Car C11:1-OH, hydroxy undecenoyl carnitine; 6β-OH cortisol, 6β-hydroxy cortisol, 16α-OH TS, 16α-hydroxy testosterone sulfate; 16α-OH AS, 16α-hydroxy androsterone sulfate.

Data are presented as fold-change *versus* control phase; increased with statistical significance (▲$P < 0.001$, ▲$P < 0.05$) in the induction phase, decreased with statistical significance (▼$P < 0.001$, ▼$P < 0.05$) in the inhibition phase

Correlations of CYP3A markers with midazolam clearance

To assess the utility of the 8 metabolites as endogenous CYP3A activity markers further, we investigated the correlation between midazolam clearance and each endogenous marker. Log-transformed urinary concentrations were highly and significantly ($P < 0.001$) correlated with log-transformed midazolam clearance (**Figure 24**).

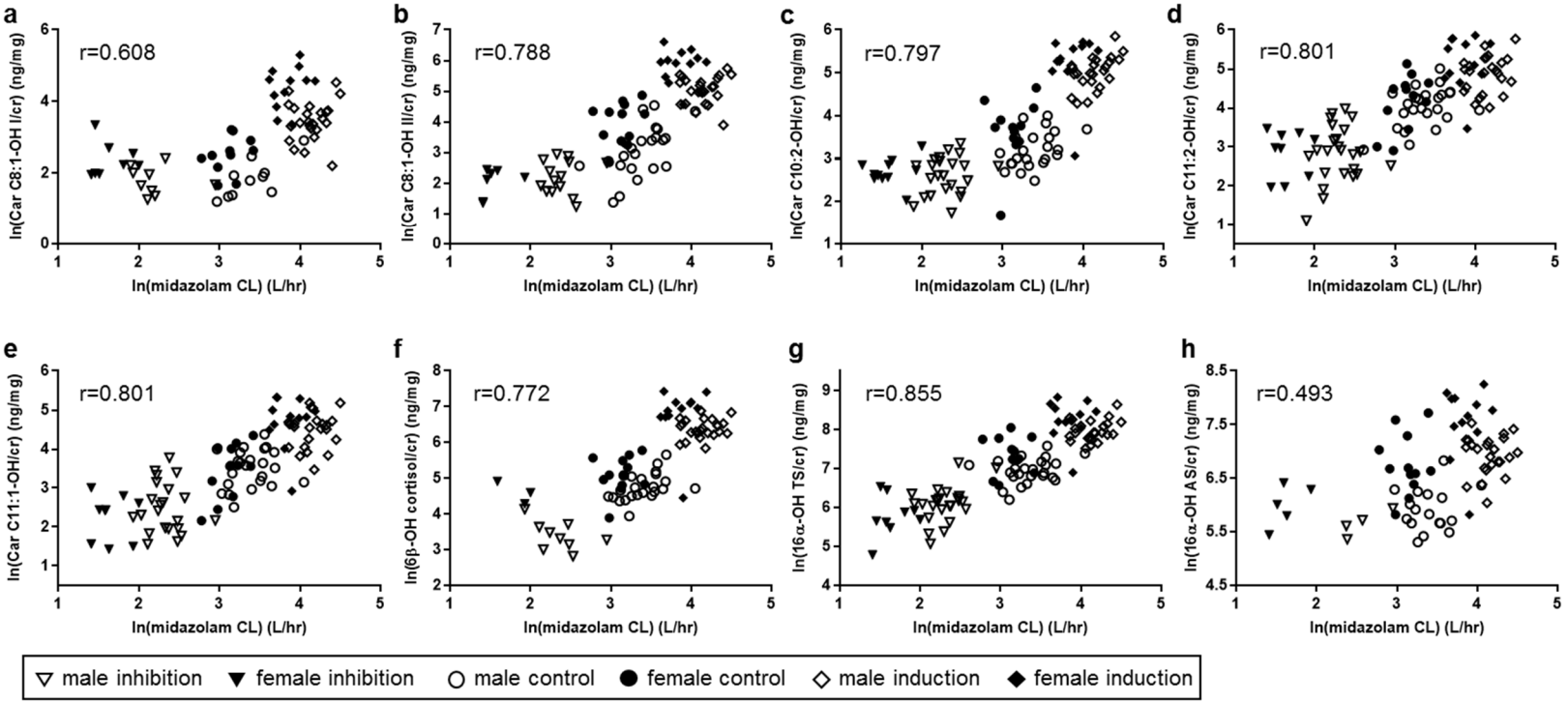

Figure 24. Correlation between midazolam clearance and (a) Car C8:1-OH I/Cr, (b) Car C8:1-OH II/Cr, (c) Car C10:2-OH/Cr, (d) Car C11:2-OH/Cr, (e) Car C11:1-OH/Cr, (f) 6β-OH cortisol/Cr, (g) 16α-OH TS/Cr, and (h) 16α-OH AS/Cr.

Construction of prediction model for midazolam clearance

The urine metabolites that significantly correlated with midazolam clearance were considered as covariates for the midazolam-clearance prediction model. Backward elimination was used to select variables (for details, refer to **Table 7 and 8**). Gender, Car C8:1-OH II, Car C10:2-OH, Car C11:2-OH, and 6β-OH-cortisol were selected as final covariates. The final model was as follows:

$$\text{Ln(clearance)} = 1.4443 - 0.5559 \cdot \text{gender}^{\dagger} + 0.1637 \cdot \ln(\text{Car C8:1-OH II/Cr} + 1) + 0.09661 \cdot \ln(\text{Car C10:2-OH/Cr}+1) + 0.1261 \cdot \ln(\text{Car C11:2-OH/Cr} + 1) + 0.1191 \cdot \ln(6\beta\text{-OH cortisol/Cr} + 1)$$

†male = 0, female = 1

The final model fitted the data well, with high correlation coefficient (r^2 = 0.911) as shown in **Figure 25**. Spaghetti plots of the predicted midazolam clearance values versus the measured midazolam clearance values in CYP3A-inhibition and control phases (**Figure 26**) and CYP3A-control and induction phases (**Figure 27**) were presented.

Table 7. Mixed effects model results for prediction of midazolam clearance

Variable	Parameter Estimate	Standard Error	DF	t- value	*P*
Intercept	1.4443	0.119	34	12.14	<.0001
Gender	-0.5559	0.07392	68	-7.52	<.0001
ln(Car C8:1-OH II/Cr+1)	0.1637	0.03012	68	5.44	<.0001
ln(Car C10:2-OH/Cr+1)	0.09661	0.0406	68	2.38	0.0201
ln(Car C11:2-OH/Cr+1)	0.1261	0.04255	68	2.96	0.0042
ln(6β-OH cortisol/Cr+1)	0.1191	0.02161	68	5.51	<.0001

Table 8. Model selection process for prediction of midazolam clearance to meet the lowest Akaike's information criterion (AIC) values

Model	Covariate	Eliminated covariate	AIC
1	CYP, NR, Gender, Car C8:1-OH I, Car C8:1-OH II, Car C10:2-OH, Car C11:2-OH, Car C11:1-OH, 6β-OH cortisol, 16a-OH TS, 16a-OH AS	16α-OH AS	84.8
2	CYP, NR, Gender, Car C8:1-OH I, Car C8:1-OH II, Car C10:2-OH, Car C11:2-OH, Car C11:1-OH, 6β-OH cortisol, 16a-OH TS	Car C8:1-OH I	80.0
3	CYP, NR, Gender, Car C8:1-OH II, Car C10:2-OH, Car C11:2-OH, Car C11:1-OH, 6β-OH cortisol, 16a-OH TS	CYP	76.2
4	NR, Gender, Car C8:1-OH II, Car C10:2-OH, Car C11:2-OH, Car C11:1-OH, 6β-OH cortisol, 16a-OH TS	16α-OH TS	72.6
5	NR, Gender, Car C8:1-OH II, Car C10:2-OH, Car C11:2-OH, Car C11:1-OH, 6β-OH cortisol	Car C11:1-OH	69.5
6	NR, Gender, Car C8:1-OH II, Car C10:2-OH, Car C11:2-OH, 6β-OH cortisol	NR	66.6
Final	**Gender, Car C8:1-OH II, Car C10:2-OH, Car C11:2-OH, 6β-OH cortisol**		

Every marker is corrected by creatinine concentration. CYP, CYP3A5 genotype; NR, NR1I2 genotype.

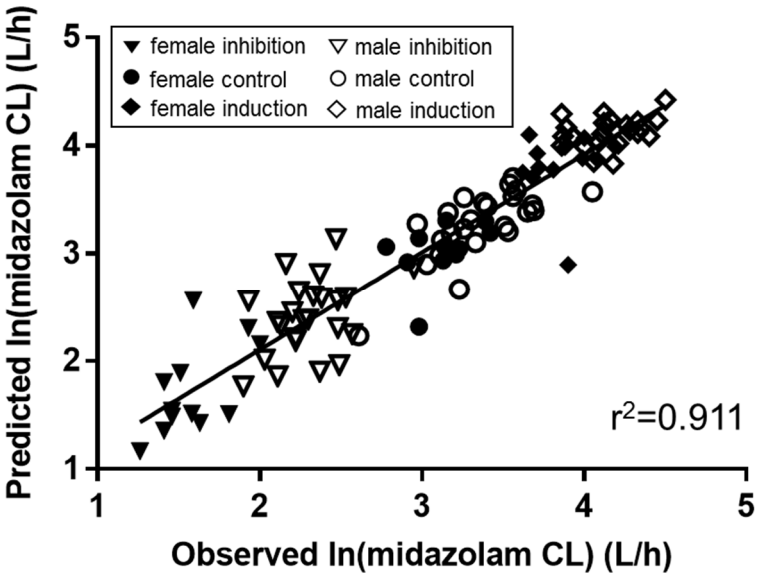

Figure 25. Scatter plot of the predicted midazolam clearance values derived from ln(clearance) = 1.4443 – 0.5559 · gender + 0.1637 · ln(Car C8:1-OH II/Cr + 1) + 0.09661 · ln(Car C10:2-OH/Cr + 1) + 0.1261 · ln(Car C11:2-OH/Cr + 1) + 0.1191 · ln(6β-OH cortisol/Cr + 1) *versus* the measured midazolam clearance values in both males and females

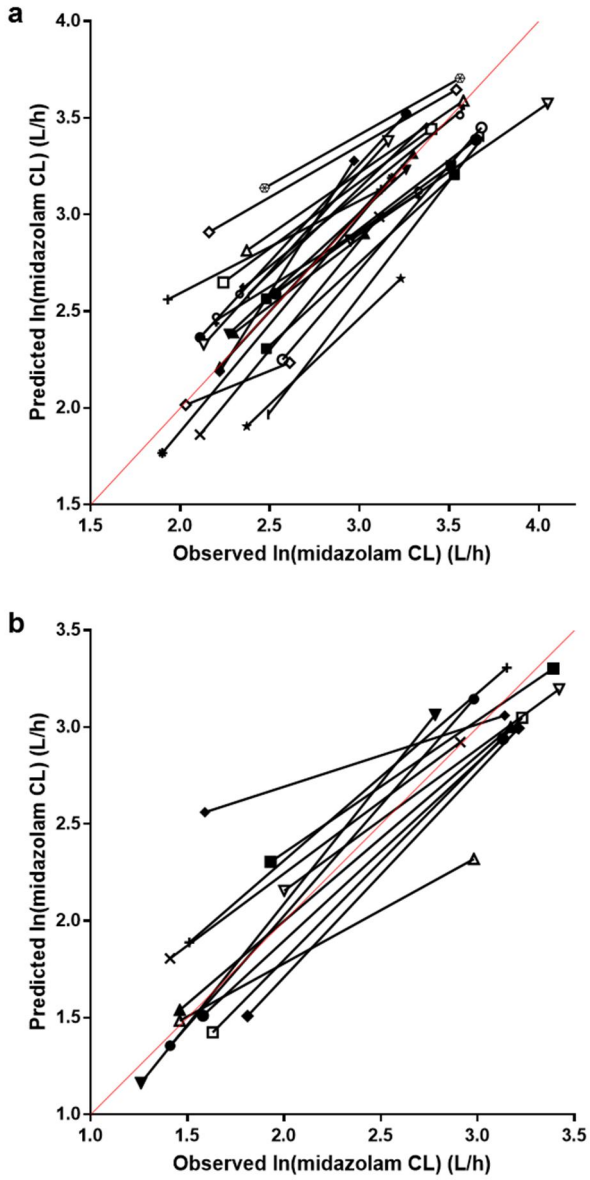

Figure 26. Spaghetti plot of the predicted midazolam clearance values versus the measured midazolam clearance values in CYP3A-inhibition and control phases of (a) males and (b) females

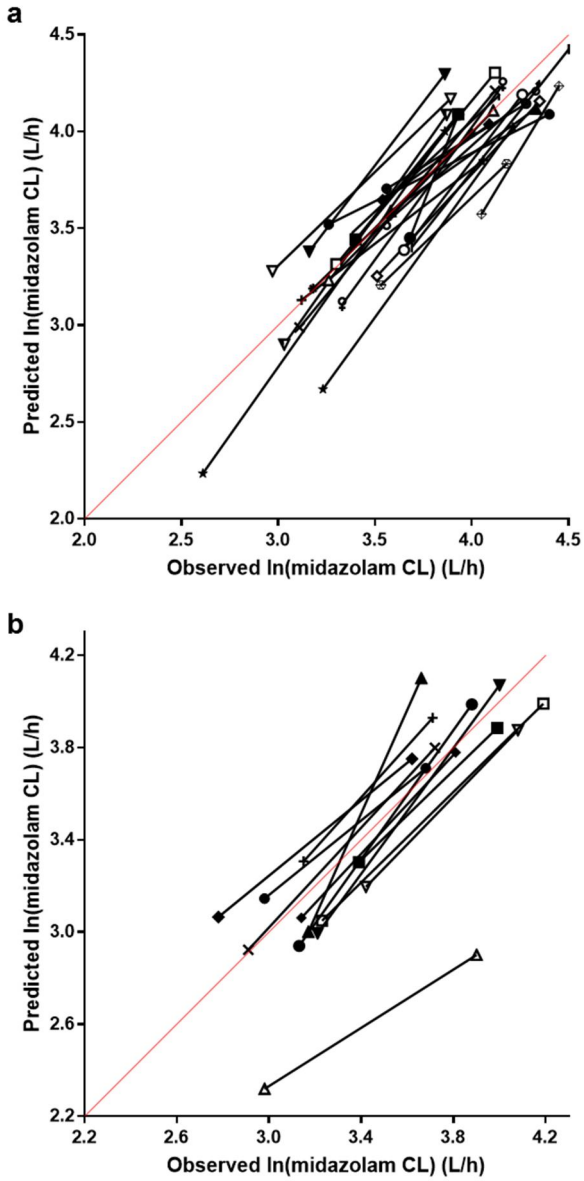

Figure 27. Spaghetti plot of the predicted midazolam clearance values versus the measured midazolam clearance values in CYP3A-control and induction phases of (a) males and (b) females

Concentration differences of biomarkers between CYP3A5*3 genotype

To evaluate the selectivity with regards to CYP3A5, we analyzed the differences in concentrations of each biomarker between the CYP3A5*3 genotype groups during any of the three study phases in each female and male subject, as outlined in the **Table 9**. The levels of the greater part of acylcarnitines, 6β-OH cortisol and 16α-OH AS, did not differ between the CYP3A5 genotype groups during any of the three study periods, with the exception of CYP3A5*3/*3, which exhibited lower levels of Car C10:2-OH, Car C11:1-OH, and 16α-OH TS than CYP3A5 *1/*3 in some CYP3A activity phases of male subjects ($P < 0.05$). This result suggested that some MCFAs (C10:2 and C11:1) and testosterone may be metabolized by CYP3A5 as well as CYP3A4.

Table 9. Differences in concentrations of CYP3A markers between CYP3A5*3 genotype groups

Metabolites	CYP3A activity phases	Male			Female			
		*1*3 (N=10)	*3*3 (N=14)	P	*1*1 (N=1)	*1*3 (N=3)	*3*3 (N=8)	P
Car C8:1-OH I (ng/mg cr)	Inhibition	1.45 ± 3.36	2.42 ± 2.89	0.34	0.31	2.05 ± 3.54	10.22 ± 8.04	0.09
	Control	2.61 ± 5.58	2.6 ± 3.3	0.51	12.79	15.07 ± 7.51	10.09 ± 7.62	0.59
	Induction	38.53 ± 24.08	33.05 ± 16.65	0.80	96.31	71.84 ± 26.94	98.19 ± 58.48	0.90
Car C8:1-OH II (ng/mg cr)	Inhibition	7.75 ± 7.26	3.70 ± 4.72	0.19	2.68	6.41 ± 5.58	3.94 ± 4.1	0.45
	Control	30.2 ± 21.03	25.35 ± 27.69	0.21	28.30	84.54 ± 19.72	59.4 ± 39.84	0.28
	Induction	191.65 ± 74.34	149.88 ± 57.06	0.19	520.12	387.29 ± 19.25	377.7 ± 209.9	0.58
Car C10:2-OH (ng/mg cr)	Inhibition	16.53 ± 6.81	10.94 ± 5.59	0.06	12.06	14.86 ± 2.73	12.75 ± 7.59	0.77
	Control	26.67 ± 11.99	23.81 ± 13.98	0.40	40.55	48.42 ± 24.93	44.89 ± 29.33	0.99
	Induction	180.82 ± 36.03	143.37 ± 70.98	0.03	259.80	166.7 ± 22.62	229.26 ± 93.72	0.15
Car C11:2-OH (ng/mg cr)	Inhibition	24.54 ± 13.08	17 ± 14.39	0.08	18.35	14.91 ± 13.42	12.87 ± 12.53	0.98
	Control	75.09 ± 35.16	52.33 ± 22.1	0.06	95.17	91.6 ± 74.74	69.52 ± 37.1	0.71
	Induction	156.88 ± 79.11	134.96 ± 56.34	0.84	276.62	179.99 ± 121.25	207.87 ± 110.96	0.68
Car C11:1-OH (ng/mg cr)	Inhibition	15.2 ± 8.66	10.8 ± 11.91	0.10	10.22	6.98 ± 6.04	7.23 ± 7.45	0.99
	Control	44.36 ± 19.77	27.08 ± 13.35	0.03	34.32	32.26 ± 23.39	38.95 ± 23.57	0.94
	Induction	106.9 ± 41.43	87.85 ± 39.15	0.37	125.51	115.82 ± 79.52	131.41 ± 58.35	0.90
6β-OH cortisol (ng/mg cr)	Inhibition	9.22 ± 15.32	13.36 ± 19.14	0.71	NQ	44.76 ± 77.53	21.24 ± 39.99	0.74
	Control	147.66 ± 65.69	98.29 ± 41.59	0.08	111.16	208.59 ± 75.61	180.07 ± 88.13	0.42
	Induction	684.42 ± 160.71	566.26 ± 147.82	0.14	1040.76	1011.52 ± 203.62	1074.81 ± 510.83	0.78

16α-OH TS (ng/mg cr)	Inhibition	619.09 ± 329.73	397.43 ± 119.26	0.03	274.95	440.04 ± 381.96	207.98 ± 150.1	0.59
	Control	1263.6 ± 386.91	951.56 ± 244.66	0.03	3145.86	1836.61 ± 469.92	1481.74 ± 678.16	0.21
	Induction	3555.96 ± 936.78	2601.26 ± 550.38	0.01	3697.40	5395.64 ± 1628.67	3870.33 ± 1626.79	0.48
16α-OH AS (ng/mg cr)	Inhibition	95.56 ± 156.09	15.06 ± 56.34	0.31	NQ	339.23 ± 309.25	137.44 ± 207.82	0.34
	Control	280.26 ± 332.24	283.12 ± 150.97	0.89	1471.33	796.07 ± 333.79	1019.72 ± 695.85	0.60
	Induction	1161.31 ± 361.13	1024.25 ± 356.13	0.29	2120.74	2290.28 ± 829.43	2188.42 ± 1153.79	0.99

DISCUSSION

Using global metabolomics, we identified ω- or (ω-1)-hydroxy-unsaturated medium-chain acylcarnitines as novel urinary biomarkers for hepatic CYP3A activity in both inhibition and induction phases in male and female subjects. In principle, unsaturated MCFAs are generated through β-oxidation in the mitochondria, and a small amount of oxidized MCFAs escapes from the mitochondria and are converted in the cytosol by carnitine palmitoyl transferase I to their acylcarnitines, which are secreted in the urine [25, 26]. The current study clearly showed that the urinary levels of acylcarnitines, including hydroxylated unsaturated MCFAs, highly correlated with midazolam clearance. Regioselective ω- and (ω-1)-hydroxylation of unsaturated MCFAs by CYP3A4 as well as CYP4 members was observed in *in vitro*.

A previous study revealed that CYP4 members are responsible for fatty acid ω-hydroxylation among the CYP family [27]. To determine which CYP450 contributes to phytanic acid ω-hydroxylation in human liver microsomes, they incubated human liver microsomes with a number of CYP450 subfamily selective inhibitors, and found that substantial inhibition of phytanic acid ω-hydroxylation was only found with 17-octadecynoic acid, diethyldithiocarbamate, and ketoconazole, which are specific inhibitors of CYP4, CYP2E1 and CYP3A4 family members, respectively. However, CYP2E1 was verified that it has no ω-hydroxylation activity by performing incubations with supersomes containing CYP2E1. Another previous study

showed that CYP2E1 hydroxylated saturated fatty acids specifically at the (ω-1) position [28]. Thus, we considered CYP3A4 and CYP4 families for *in vitro* study.

CYP4 proteins catalyze the ω- and (ω-1)-hydroxylation of saturated, branched-chain, and unsaturated fatty acids, including the physiologically important eicosanoids, prostaglandins, leukotrienes, and arachidonic acid [28, 29]. In mammals, 6 CYP4 subfamilies have been identified: CYP4A, CYP4B, CYP4F, CYP4V, CYP4X, and CYP4Z [29]. CYP4A11, CYP4F2, and CYP4F3B ω-hydroxylate fatty acids in the human liver and kidneys [30]. Given that CYP4A11 and 4F2 contribute to the metabolism of MCFAs and are expressed at much higher levels than CYP3A4 in human kidneys [31], the contribution of renal CYP4 metabolism to renally excreted biomarkers of acylcarnitines is unclear. However, the amount of CYP4 protein in the human body is relatively low compared to that of CYP3A4, and MCFAs are formed mainly in the liver [32]; thus, the contribution of CYP4 members to the overall production of hydroxylated acylcarnitine markers should be minor. Furthermore, CYP3A4 had lower Km and higher Vmax/Km values than CYP4A11 and CYP4F2, indicating that CYP3A4 is the most efficient enzyme for 2-octenoic acid ω- and (ω-1)-hydroxylation. Therefore, the ω- and (ω-1)-hydroxylated acylcarnitines are potential biomarkers for CYP3A activity.

Additionally, potential inhibitory or inductive effects of ketoconazole and rifampicin on CYP4 enzymes should be considered. A previous study showed CYP4F12 to be induced in human hepatocytes treated with rifampicin, a pregnane X receptor agonist [33]. Therefore, inhibitory effects of

ketoconazole on CYP4A11 and CYP4F2 were assessed to rule out that CYP4 enzymes were affected in the ketoconazole-mediated inhibition phase. Based on IC50 values, ketoconazole did hardly or not inhibit CYP4A11 and CYP4F2.

The prediction of regioselectivity in CYP3A4-mediated metabolism is crucial for drug discovery and development. Four major metabolic reactions are mediated by CYP3A4; aliphatic hydroxylation, N-dealkylation, O-dealkylation, and aromatic hydroxylation. In our study, CYP3A4 showed regioselectivity for ω- and (ω-1)-hydroxylation of unsaturated MCFAs. Consistent herewith, a previous study reported that the ω- and (ω-1)-hydroxylation of fatty acids by CYP4A and 2E1 decreased with increasing alkyl-chain length of saturated fatty acids, while the reverse was observed for double bonds [34].

Because CYP3A is localized in the liver and small intestine, CYP3A activity contributes extensively to first-pass metabolism of multiple drugs. One of the important considerations for the use of CYP3A as an endogenous biomarker is that it will likely reflect hepatic, but not intestinal CYP3A levels [35]. MCFAs consist of 8–12 carbons and are found in palm oil and other food types. Dietary fat medium-chain triacylglycerols (MCT) are MCFA esters of glycerol and are hydrolyzed rapidly to MCFAs, which are readily absorbed by the liver for β-oxidation [36, 37]. Thus, hydroxylated medium-chain acylcarnitines might reflect intestinal as well as hepatic CYP3A activity; however, this remains to be validated. In addition, MCFAs are of nutritional interest because they are easily absorbed from dietary MCTs, and

MCFAs/MCTs diminish fat deposition through enhancement of thermogenesis and fat oxidation in animals [38] and humans [39, 40]. Additionally, MCFAs/MCTs offer the therapeutic advantage of preserving insulin sensitivity in animal models and patients with type 2 diabetes [41]. Our results suggest that the influence of MCFA hydroxylation by CYP3A on these health benefits should be evaluated. The value of hydroxy acylcarnitine as a urine biomarker for CYP3A activity requires further validation, e.g. in subjects with different inhibition and induction state capabilities or under oral administration of CYP3A probe drug to confirm whether intestinal CYP3A activity can be evaluated.

Consistent with our previously reported models for predicting midazolam clearance using steroid markers (4,5), urinary 6β-OH cortisol was selected as a CYP3A marker in the final model showing a strong correlation with midazolam clearance (r = 0.772). Along with 6β-OH cortisol, the novel 3-hydroxy acylcarnitine CYP3A markers as covariates in our model reflected the extent of CYP3A activity in both genders, with high predictability (r^2 = 0.911).

Elevations of hydroxy testosterone sulfate and hydroxy androsterone sulfate have been observed following rifampicin administration [42]. Furthermore, significant changes in urinary metabolites [11] and metabolite ratio of 16α-hydroxy testosterone and 16α-hydroxy testosterone/testosterone [10] have been observed in the CYP3A-inhibited phase as compared to the control phase. In contrast, 16α-hydroxy testosterone/testosterone was not significantly changed in the CYP3A-induced phase as compared to the control

phase [10], but 16α-OH TS was significantly altered by both CYP3A inhibition and induction in this study, which means that sulfotransferase (SULT) 2A1, in addition to CYP3A, contributes to the metabolism of testosterone.

We constructed a model that integrated data from previous steroid markers (6β-OH cortisol/cortisol and 6β-OH cortisone) [22] and acylcarnitine markers of this study. Backward elimination was used to select variables (for details, refer to **Table 10 and 11**). Gender, Car C8:1-OH II, Car C11:2-OH, 6β-OH-cortisol/cortisol, and 6β-OH-cortisone/cortisone were selected as final covariates (**Figure 28**). The final equation was as follows:

$$\text{Ln(clearance)} = 1.3681 - 0.6194 \cdot \text{gender}^{\dagger} + 0.1309 \cdot \ln(\text{Car C8:1-OH II/Cr} + 1) + 0.1300 \cdot \ln(\text{Car C11:2-OH/Cr} + 1) + 0.5608 \cdot \ln(6\beta\text{-OH cortisol/cortisol}) - 0.6993 \cdot \ln(6\beta\text{-OH cortisone/cortisone})$$

†male = 0, female = 1

The integrated model showed higher correlation coefficient (r^2 = 0.937) and lower AIC values (43.1) compared to the final model in this study (r^2=0.911 and AIC values = 66.6).

In conclusion, using a global metabolomics approach, we identified urinary hydroxy acylcarnitines as novel CYP3A biomarkers and found that CYP3A4 efficiently catalyzes the ω- and (ω-1)-hydroxylation of unsaturated MCFAs. Using the urinary markers of hydroxy acylcarnitines and 6β-OH cortisol, we established a predictive model for hepatic CYP3A activity under the inhibition and induction states in males and females. The selected markers

of hepatic CYP3A activity and the proposed model can be applied to predict DDI mediated by CYP3A.

Table 10. Mixed-effect model results of integrated data

Effect	Estimate	Standard Error	DF	t Value	Pr > |t|
Intercept	1.3681	0.1011	34	13.53	<.0001
Sex	-0.6194	0.07935	68	-7.81	<.0001
ln (Car C8:1-OH II/Cr)	0.1309	0.02865	68	4.57	<.0001
ln (Car C11:2-OH/Cr)	0.1300	0.03764	68	3.45	0.0001
ln (6β-OH-Cortisol/Cortisol)	0.5608	0.07263	68	7.72	<.0001
ln (6β-OH-Cortisone/Cortisone)	-0.6993	0.1771	68	-3.95	0.0002

Table 11. Model selection process of integrated model for prediction of midazolam clearance to meet the lowest Akaike's information criterion (AIC) values

Model	Covariate	Eliminated covariate	AIC
Initial	Gender, Age, CYP, Car C8:1-OH II/Cr, Car C10:2-OH/Cr, Car C11:2-OH/Cr, Car C11:1-OH/Cr, 6β-OH-Cortisol/Cortisol, 6β-OH Cortisone/Cortisone		61.2
1	Gender, CYP, Car C8:1-OH II/Cr, Car C10:2-OH/Cr, Car C11:2-OH/Cr, Car C11:1-OH/Cr, 6β -OH-Cortisol/Cortisol, 6β-OH Cortisone/Cortisone	Age	54.2
2	Gender, Car C8:1-OH II/Cr, Car C10:2-OH/Cr, Car C11:2-OH/Cr, Car C11:1-OH/Cr, 6β -OH-Cortisol/Cortisol, 6β-OH Cortisone/Cortisone	CYP	50.1
3	Gender, Car C8:1-OH II/Cr, Car C11:2-OH/Cr, Car C11:1-OH/Cr, 6β-OH-Cortisol/Cortisol, 6β-OH Cortisone/Cortisone	Car C10:2-OH/Cr	46.0
4	Gender, Car C8:1-OH II/Cr, Car C11:2-OH/Cr, 6β-OH-Cortisol/Cortisol, 6β-OH Cortisone/Cortisone	Car C11:1-OH/Cr	43.1
Final	**Gender, Car C8:1-OH II/Cr, Car C11:2-OH/Cr, 6β-OH Cortisone/Cortisol, 6β-OH-Cortisol/Cortisone**		

Every marker is corrected by creatinine concentration. CYP, CYP3A5 genotype

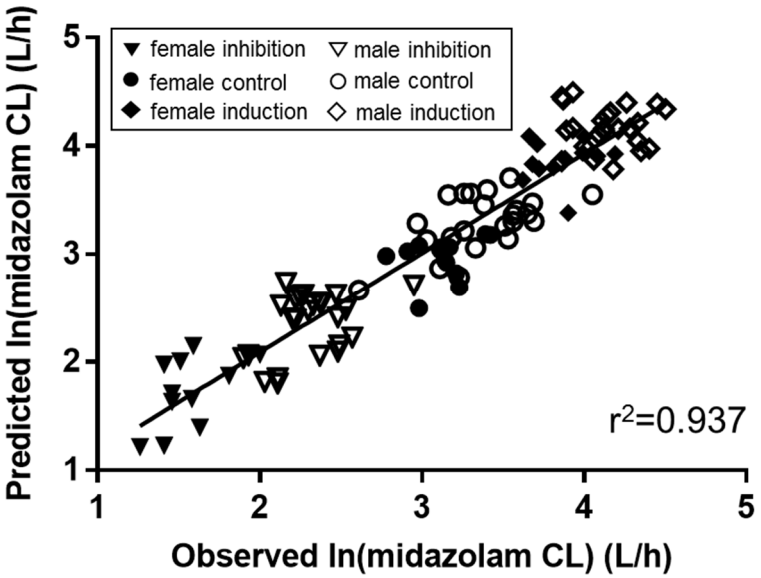

Figure 28. Scatter plot of the predicted midazolam clearance values derived from ln(clearance) = 1.3681 – 0.6194 · gender + 0.1309 · ln(Car C8:1-OH II/Cr + 1) + 0.1300 · ln(Car C11:2-OH/Cr + 1) + 0.5608 · ln(6β-OH cortisol/cortisol) – 0.6993 · ln(6β-OH cortisone/cortisone) *versus* the measured midazolam clearance values in both males and females.

REFERENCES

1. Lehmann, J.M., McKee, D.D., Watson, M.A., Willson, T.M., Moore, J.T., and Kliewer, S.A. (1998). The human orphan nuclear receptor PXR is activated by compounds that regulate CYP3A4 gene expression and cause drug interactions. J Clin Invest *102*, 1016-1023.
2. Stevens, J.C., Hines, R.N., Gu, C., Koukouritaki, S.B., Manro, J.R., Tandler, P.J., and Zaya, M.J. (2003). Developmental expression of the major human hepatic CYP3A enzymes. The Journal of pharmacology and experimental therapeutics *307*, 573-582.
3. Kang, Y.S., Park, S.Y., Yim, C.H., Kwak, H.S., Gajendrarao, P., Krishnamoorthy, N., Yun, S.C., Lee, K.W., and Han, K.O. (2009). The CYP3A4*18 genotype in the cytochrome P450 3A4 gene, a rapid metabolizer of sex steroids, is associated with low bone mineral density. Clin Pharmacol Ther *85*, 312-318.
4. Elens, L., Bouamar, R., Hesselink, D.A., Haufroid, V., van Gelder, T., and van Schaik, R.H. (2012). The new CYP3A4 intron 6 C>T polymorphism (CYP3A4*22) is associated with an increased risk of delayed graft function and worse renal function in cyclosporine-treated kidney transplant patients. Pharmacogenet Genomics *22*, 373-380.
5. Diczfalusy, U., Miura, J., Roh, H.K., Mirghani, R.A., Sayi, J., Larsson, H., Bodin, K.G., Allqvist, A., Jande, M., Kim, J.W., et al. (2008). 4Beta-hydroxycholesterol is a new endogenous CYP3A marker: relationship to CYP3A5 genotype, quinine 3-hydroxylation and sex in Koreans, Swedes and Tanzanians. Pharmacogenet Genomics *18*, 201-208.
6. Lehmann, J.M., McKee, D.D., Watson, M.A., Willson, T.M., Moore, J.T., and Kliewer, S.A. (1998). The human orphan nuclear receptor PXR is activated by compounds that regulate CYP3A4 gene expression and cause drug interactions. J Clin Invest *102*, 1016-1023.
7. Schmiedlin-Ren, P., Thummel, K.E., Fisher, J.M., Paine, M.F., and Watkins, P.B. (2001). Induction of CYP3A4 by 1 alpha,25-dihydroxyvitamin D-3 is human cell line-specific and is unlikely to involve pregnane X receptor. Drug Metabolism and Disposition *29*, 1446-1453.
8. Wang, K., Chen, S., Xie, W., and Wan, Y.J.Y. (2008). Retinoids induce cytochrome P450 3A4 through RXR/VDR-mediated pathway. Biochem Pharmacol *75*, 2204-2213.
9. Zhang, L., Zhang, Y.D., Zhao, P., and Huang, S.M. (2009). Predicting drug-drug interactions: an FDA perspective. Aaps J *11*, 300-306.
10. Shin, K.H., Choi, M.H., Lim, K.S., Yu, K.S., Jang, I.J., and Cho,

J.Y. (2013). Evaluation of endogenous metabolic markers of hepatic CYP3A activity using metabolic profiling and midazolam clearance. Clinical pharmacology and therapeutics *94*, 601-609.
11. Shin, K.H., Ahn, L.Y., Choi, M.H., Moon, J.Y., Lee, J., Jang, I.J., Yu, K.S., and Cho, J.Y. (2016). Urinary 6beta-Hydroxycortisol/Cortisol Ratio Most Highly Correlates With Midazolam Clearance Under Hepatic CYP3A Inhibition and Induction in Females: A Pharmacometabolomics Approach. AAPS J *18*, 1254-1261.
12. Kasichayanula, S., Boulton, D.W., Luo, W.L., Rodrigues, A.D., Yang, Z., Goodenough, A., Lee, M., Jemal, M., and LaCreta, F. (2014). Validation of 4beta-hydroxycholesterol and evaluation of other endogenous biomarkers for the assessment of CYP3A activity in healthy subjects. Br J Clin Pharmacol *78*, 1122-1134.
13. Galteau, M.M., and Shamsa, F. (2003). Urinary 6beta-hydroxycortisol: a validated test for evaluating drug induction or drug inhibition mediated through CYP3A in humans and in animals. Eur J Clin Pharmacol *59*, 713-733.
14. Bjorkhem-Bergman, L., Backstrom, T., Nylen, H., Ronquist-Nii, Y., Bredberg, E., Andersson, T.B., Bertilsson, L., and Diczfalusy, U. (2013). Comparison of endogenous 4beta-hydroxycholesterol with midazolam as markers for CYP3A4 induction by rifampicin. Drug Metab Dispos *41*, 1488-1493.
15. Chan, K.C., Lit, L.C., Law, E.L., Tai, M.H., Yung, C.U., Chan, M.H., and Lam, C.W. (2004). Diminished urinary free cortisol excretion in patients with moderate and severe renal impairment. Clin Chem *50*, 757-759.
16. Furuta, T., Suzuki, A., Mori, C., Shibasaki, H., Yokokawa, A., and Kasuya, Y. (2003). Evidence for the validity of cortisol 6 beta-hydroxylation clearance as a new index for in vivo cytochrome P450 3A phenotyping in humans. Drug Metab Dispos *31*, 1283-1287.
17. Bodin, K., Andersson, U., Rystedt, E., Ellis, E., Norlin, M., Pikuleva, I., Eggertsen, G., Bjorkhem, I., and Diczfalusy, U. (2002). Metabolism of 4 beta -hydroxycholesterol in humans. J Biol Chem *277*, 31534-31540.
18. Diczfalusy, U., Kanebratt, K.P., Bredberg, E., Andersson, T.B., Bottiger, Y., and Bertilsson, L. (2009). 4beta-hydroxycholesterol as an endogenous marker for CYP3A4/5 activity. Stability and half-life of elimination after induction with rifampicin. Br J Clin Pharmacol *67*, 38-43.
19. Wang, Z.C., Lin, Y.S., Zheng, X.E., Senn, T., Hashizume, T., Scian, M., Dickmann, L.J., Nelson, S.D., Baillie, T.A., Hebert, M.F., et al. (2012). An Inducible Cytochrome P450 3A4-Dependent Vitamin D Catabolic Pathway. Mol Pharmacol *81*, 498-509.

20. Hayes, M.A., Li, X.Q., Gronberg, G., Diczfalusy, U., and Andersson, T.B. (2016). CYP3A Specifically Catalyzes 1beta-Hydroxylation of Deoxycholic Acid: Characterization and Enzymatic Synthesis of a Potential Novel Urinary Biomarker for CYP3A Activity. Drug Metab Dispos *44*, 1480-1489.
21. Lee, J., Kim, A.H., Yi, S., Lee, S., Yoon, S.H., Yu, K.S., Jang, I.J., and Cho, J.Y. (2017). Distribution of Exogenous and Endogenous CYP3A Markers and Related Factors in Healthy Males and Females. Aaps J.
22. Shin, K.H., Ahn, L.Y., Choi, M.H., Moon, J.Y., Lee, J., Jang, I.J., Yu, K.S., and Cho, J.Y. (2016). Urinary 6 beta-Hydroxycortisol/Cortisol Ratio Most Highly Correlates With Midazolam Clearance Under Hepatic CYP3A Inhibition and Induction in Females: A Pharmacometabolomics Approach. Aaps J *18*, 1254-1261.
23. Lee, J., Kim, A.H., Yi, S., Lee, S., Yoon, S.H., Yu, K.S., Jang, I.J., and Cho, J.Y. (2017). Distribution of Exogenous and Endogenous CYP3A Markers and Related Factors in Healthy Males and Females. Aaps J *19*, 1196-1204.
24. Hardwick, J.P. (2008). Cytochrome P450 omega hydroxylase (CYP4) function in fatty acid metabolism and metabolic diseases. Biochem Pharmacol *75*, 2263-2275.
25. Wanders, R.J.A., Komen, J., and Kemp, S. (2011). Fatty acid omega-oxidation as a rescue pathway for fatty acid oxidation disorders in humans. Febs J *278*, 182-194.
26. Chen, J., Wang, W., Lv, S., Yin, P., Zhao, X., Lu, X., Zhang, F., and Xu, G. (2009). Metabonomics study of liver cancer based on ultra performance liquid chromatography coupled to mass spectrometry with HILIC and RPLC separations. Anal Chim Acta *650*, 3-9.
27. Wanders, R.J.A., and Komen, J.C. (2006). Identification of the cytochrome P450 enzymes responsible for the omega-hydroxylation of phytanic acid: Implications for Refsum disease. J Inherit Metab Dis *29*, 77-77.
28. Adas, F., Salaun, J.P., Berthou, F., Picart, D., Simon, B., and Amet, Y. (1999). Requirement for omega and (omega-1)-hydroxylations of fatty acids by human cytochromes P450 2E1 and 4A11. J Lipid Res *40*, 1990-1997.
29. Hardwick, J.P. (2008). Cytochrome P450 omega hydroxylase (CYP4) function in fatty acid metabolism and metabolic diseases. Biochem Pharmacol *75*, 2263-2275.
30. Hsu, M.H., Savas, U., Griffin, K.J., and Johnson, E.F. (2007). Human cytochrome P450 family 4 enzymes: Function, genetic variation and regulation. Drug Metab Rev *39*, 515-538.
31. Knights, K.M., Rowland, A., and Miners, J.O. (2013). Renal drug metabolism in humans: the potential for drug-endobiotic

interactions involving cytochrome P450 (CYP) and UDP-glucuronosyltransferase (UGT). Br J Clin Pharmacol *76*, 587-602.
32. Schonfeld, P., and Wojtczak, L. (2016). Short- and medium-chain fatty acids in energy metabolism: the cellular perspective. J Lipid Res *57*, 943-954.
33. Hariparsad, N., Chu, X., Yabut, J., Labhart, P., Hartley, D.P., Dai, X., and Evers, R. (2009). Identification of pregnane-X receptor target genes and coactivator and corepressor binding to promoter elements in human hepatocytes. Nucleic Acids Res *37*, 1160-1173.
34. Adas, F., Salaun, J.P., Berthou, F., Picart, D., Simon, B., and Amet, Y. (1999). Requirement for omega and (omega;-1)-hydroxylations of fatty acids by human cytochromes P450 2E1 and 4A11. J Lipid Res *40*, 1990-1997.
35. Tracy, T.S., Chaudhry, A.S., Prasad, B., Thummel, K.E., Schuetz, E.G., Zhong, X.B., Tien, Y.C., Jeong, H., Pan, X., Shireman, L.M., et al. (2016). Interindividual Variability in Cytochrome P450-Mediated Drug Metabolism. Drug Metab Dispos *44*, 343-351.
36. Takeuchi, H., Sekine, S., Kojima, K., and Aoyama, T. (2008). The application of medium-chain fatty acids: edible oil with a suppressing effect on body fat accumulation. Asia Pac J Clin Nutr *17*, 320-323.
37. Nagao, K., and Yanagita, T. (2010). Medium-chain fatty acids: Functional lipids for the prevention and treatment of the metabolic syndrome. Pharmacol Res *61*, 208-212.
38. Baba, N., Bracco, E.F., and Hashim, S.A. (1987). Role of brown adipose tissue in thermogenesis induced by overfeeding a diet containing medium chain triglyceride. Lipids *22*, 442-444.
39. St-Onge, M.P., and Jones, P.J. (2002). Physiological effects of medium-chain triglycerides: potential agents in the prevention of obesity. J Nutr *132*, 329-332.
40. St-Onge, M.P., Ross, R., Parsons, W.D., and Jones, P.J. (2003). Medium-chain triglycerides increase energy expenditure and decrease adiposity in overweight men. Obes Res *11*, 395-402.
41. Han, J.R., Deng, B., Sun, J., Chen, C.G., Corkey, B.E., Kirkland, J.L., Ma, J., and Guo, W. (2007). Effects of dietary medium-chain triglyceride on weight loss and insulin sensitivity in a group of moderately overweight free-living type 2 diabetic Chinese subjects. Metabolism *56*, 985-991.
42. Kim, B., Moon, J.Y., Choi, M.H., Yang, H.H., Lee, S., Lim, K.S., Yoon, S.H., Yu, K.S., Jang, I.J., and Cho, J.Y. (2013). Global metabolomics and targeted steroid profiling reveal that rifampin, a strong human PXR activator, alters endogenous urinary steroid markers. J Proteome Res *12*, 1359-1368.

국문 초록

서론: Cytochrome P450 (CYP)3A 는 주요 약물대사효소로 그 대사능을 정량적으로 측정하기 위해 probe drug 인 midazolam 을 이용해왔다. 그러나 이러한 불필요한 약물의 노출과 침습적인 샘플링 과정을 피하면서 개인의 CYP3A 대사능을 측정하기 위해 CYP3A 에 의해 특이적으로 대사되는 내인성 마커 (특히 소변 마커)를 이용하는 비침습적인 방법이 연구되었다. 이러한 CYP3A 내인성마커를 이용한 정량적 모델은 약물간 상호작용을 예측하는데 유용하다. 본 연구에서는 건강한 성인 남성 및 여성 자원자의 CYP3A 저해 및 활성 상태에서 CYP3A 의 대사능을 반영하는 새로운 대사체 마커를 발굴하고자 하였다.

방법: 건강한 성인 남성 24 명 및 여성 12 명이 3 가지 치료를 3 기에 걸쳐 정해진 순서에 따라 모두 투여 받는 형태로 다음과 같이 연구를 설계하였다; 1 기 (control)에 midazolam 투여, 2 기 (inhibition)에 ketoconazole 반복 투여 후, midazolam 투여 받았다. 3 기 (induction)에 rifampicin 반복투여 후, midazolam 을 투여하였다. 이로써 각 투여 시기의 midazolam 약동학을 평가하였다. 또한 각 시기의 12 시간 구간 소변을 수집하여, ultra-performance liquid chromatography time-of-flight mass spectrometry 를 이용한 비표적 대사체를 분석하였다. CYP3A 대사능을 반영하는 대사

체마커를 선정하기 위한 세 가지 조건은 다음과 같다; (1) control 대비 inhibition 시기에 relative intensity 의 평균값이 0.5 배 미만, (2) control 대비 induction 시기에 relative intensity 의 평균값이 2 배 초과, (3) midazolam 청소율과 relative intensity 의 상관관계 Pearson r 값이 0.7 초과. CYP 효소 반응도를 보기 위해, CYP3A4, CYP4A11, 그리고 CYP4F2 recombinant enzyme 을 이용하여 Km,, Vmax, Vmax/Km 값을 비교하였다.

결과: 본 연구를 통해 새로운 CYP3A4 대사능 마커로 5 개의 ω- or (ω-1)-hydroxylated medium-chain acylcarnitine 을 발굴하였다. Recombinant enzyme 을 이용한 CYP3A4, CYP4A11, CYP4F2 의 ω- and (ω-1)-hydroxylation 효소 반응도를 보고자 하였다. 이를 통해 CYP3A4 가 가장 낮은 Km 값과 가장 높은 Vmax/Km 값을 가지는 것을 확인하였다. 최종적으로 본 연구에서 발굴한 마커들을 이용하여 midazolam 청소율을 예측할 수 있는 모델을 도출하였다. 최종 모델은 3 개의 ω- or (ω-1)-hydroxylated medium-chain acylcarnitine, 6β-OH cortisol, gender 변수를 포함하고 있으며, 높은 예측률을 보였다 (r^2 = 0.911).

$$\begin{aligned}\text{Ln(clearance)} = {} & 1.4443 - 0.5559 \cdot \text{gender}^{\dagger} + 0.1637 \cdot \ln(\text{Car C8:1-OH II/Cr} + 1) \\ & + 0.09661 \cdot \ln(\text{Car C10:2-OH/Cr}+1) + 0.1261 \cdot \ln(\text{Car C11:2-OH/Cr} + 1) \\ & + 0.1191 \cdot \ln(6\beta\text{-OH cortisol/Cr} + 1)\end{aligned}$$

†male = 0, female = 1

결론: 비표적 대사체학을 이용하여 새로운 CYP3A 대사능 내인성마커인 hydroxy acylcarnitine 을 동정하였으며, 기존에 알려진 medium-chain fatty acid 를 대사시키는 CYP4 family 의 효소들과 비교했을 때, CYP3A4 가 CYP4 family 보다 ω- and (ω-1)-hydroxylation 효소반응이 효율적인 것을 확인하였다. 본 연구를 통해 발굴한 새로운 마커와 이로 만든 모델이 CYP3A4 관련 약물상호작용을 예측하는데 기여할 수 있을 것이다.

* 본 내용의 일부는 Clinical Pharmacology and Therapeutics 학술지 (Bora Kim, et al. CPT In press. doi: 10.1002/cpt.856)에 출판 예정된 내용임.

주요어 : CYP3A, 약물 상호작용, 정량적 모델, 비표적 대사체학, acylcarnitine, medium-chain fatty acid, ω- and (ω-1)-hydroxylation

학 번 : 2013-30608